2022

LIGNIN VALORIZATION VIA REDUCTIVE DEPOLYMERIZATION USING PROMOTED NICKEL CATALYSTS AND SUB- AND SUPERCRITICAL METHANOL

Julia Parker
University of Kentucky, julia.parker@uky.edu
Digital Object Identifier: https://doi.org/10.13023/etd.2022.454

STUDENT AGREEMENT:

I represent that my thesis or dissertation and abstract are my original work. Proper attribution has been given to all outside sources. I understand that I am solely responsible for obtaining any needed copyright permissions. I have obtained needed written permission statement(s) from the owner(s) of each third-party copyrighted matter to be included in my work, allowing electronic distribution (if such use is not permitted by the fair use doctrine) which will be submitted to UKnowledge as Additional File.

I hereby grant to The University of Kentucky and its agents the irrevocable, non-exclusive, and royalty-free license to archive and make accessible my work in whole or in part in all forms of media, now or hereafter known. I agree that the document mentioned above may be made available immediately for worldwide access unless an embargo applies.

I retain all other ownership rights to the copyright of my work. I also retain the right to use in future works (such as articles or books) all or part of my work. I understand that I am free to register the copyright to my work.

REVIEW, APPROVAL AND ACCEPTANCE

The document mentioned above has been reviewed and accepted by the student's advisor, on behalf of the advisory committee, and by the Director of Graduate Studies (DGS), on behalf of the program; we verify that this is the final, approved version of the student's thesis including all changes required by the advisory committee. The undersigned agree to abide by the statements above.

Julia Parker, Student

Dr. Czarena L. Crofcheck, Major Professor

Dr. Michael Sama, Director of Graduate Studies

LIGNIN VALORIZATION VIA REDUCTIVE DEPOLYMERIZATION USING PROMOTED NICKEL CATALYSTS AND SUB- AND SUPERCRITICAL METHANOL

THESIS

A thesis submitted in partial fulfillment of the
requirements for the degree of Master of Science in the
Colleges of Agriculture and Engineering
at the University of Kentucky

By

Julia Evette Parker

Lexington, Kentucky

Co- Directors: Dr. Czarena L. Crofcheck, Professor of Biosystems and Agricultural Engineering

and Dr. Eduardo Santillan-Jimenez, Adjunct Assistant Professor of Chemistry

Lexington, Kentucky

2022

ABSTRACT OF THESIS

LIGNIN VALORIZATION VIA REDUCTIVE DEPOLYMERIZATION USING PROMOTED NICKEL CATALYSTS AND SUB- AND SUPERCRITICAL METHANOL

While lignin has been regarded as the most promising renewable feedstock for the sustainable manufacture of aromatic compounds, lignin valorization is necessary to improve the economic viability of biorefineries. Reductive catalytic fractionation (RCF), which combines delignification and lignin depolymerization into a single stage while maintaining the structure and integrity of the cellulose component, has evolved as an effective method for processing biomass.

The ability of Cu and Fe to promote the performance of a 20% Ni/alumina catalyst when converting native lignin to alkylphenols by RCF in sub- and supercritical methanol was tested. The effectiveness of lignin extraction as measured by lignin oil production, the quantity and distribution of identifiable monomers in lignin oil, and the yield of residual solids were examined.

All Ni-based catalysts tested performed similarly in terms of product distribution and monomer yields, offering improved yields of lignin oil and detectable monomers along with reduced char formation in conditions relative to blank (sans catalyst) runs. Ni-Cu catalyst in the presence of supercritical methanol, with a monomer yield of 51%, performed better than Ni-Fe and Ni-only formulations.

Several catalyst characterization methods were employed to identify the structure-activity relationships underpinning the performance of these catalysts in lignin valorization.

KEYWORDS: Lignocellulosic biomass, lignin valorization, Ni-based catalysts, reductive depolymerization, supercritical methanol

Julia Evette Parker

(Name of Student)

11/22/2022

Date

LIGNIN VALORIZATION VIA REDUCTIVE DEPOLYMERIZATION USING PROMOTED NICKEL CATALYSTS AND SUB- AND SUPERCRITICAL METHANOL

By
Julia Evette Parker

Dr. Czarena L. Crofcheck
Co-Director of Thesis

Dr. Eduardo Santillan-Jimenez
Co-Director of Thesis

Dr. Michael Sama
Director of Graduate Studies

11/22/2022
Date

DEDICATION

This thesis is dedicated to all of the negative and stressful situations that occurred during my master's program.

Thank you for giving me the opportunity to learn that the pursuit of science is not based on prestige, success, or positivity, but rather on tenacity, curiosity, and, most importantly, resiliency.

ACKNOWLEDGMENTS

I would like to express my gratitude to my research mentor, Dr. Eduardo Santillan-Jimenez, for his continuous encouragement, counsel, and wisdom. It has been a pleasure and a privilege to work with him. I would also like to thank the other members of my advisory committee: Dr. Czarena Crofcheck for all of her knowledge and guidance; Dr. Jian Shi for allowing me to utilize his lab equipment and for the essential material he taught me in class.

Many thanks to all of my colleagues, friends, faculty, and staff at the University of Kentucky's Department of Biosystems Engineering and the Center for Applied Energy Research (CAER), especially Dr. Mark Crocker, for accepting me as an undergraduate research student and for welcoming me into his lab group at CAER as a graduate researcher.

Also, thank you to Drs. Vanessa Song, Robert Pace, and Justin Mobley for all of your training and assistance. I cherish the memories we made at CAER. I'd also like to thank my other colleagues in the Biofuels and Environmental Catalysis group at CAER, Gayan Karunasinhe and C. Great Umenweke, for their assistance with data analysis, as well as their encouragement and friendship.

Thank you to my family and friends for your kindness and moral support. A special thanks to Anthony DeSana, my life partner who has been my life preserver throughout this journey. This effort would not have been possible without his unwavering love, support, and advice.

This research was partially supported by grants from the National Science Foundation with the numbers HRD 2004210 and 1922694.

TABLE OF CONTENTS

LIST OF TABLES

LIST OF FIGURES

CHAPTER 1. GENERAL INTRODUCTION

1.1 Overall significance

Most of the world's energy needs are now met by fossil fuels, making the search for sustainable alternatives to power transportation, electricity generation, and industry, one of the greatest challenges facing human societies in the twenty-first century. For instance, in the U.S. currently 79% of annual energy consumption is met with nonrenewable fossil fuels (Figure 1.1). However, the rate of increase in energy demand exceeds the rate of improvement in energy efficiency, as a result of rising population and expanding economies (Annual Energy Outlook (AEO) 2022). In addition to lowering greenhouse gas emissions, the energy source of the future must not interfere with land required for agricultural production. Biomass that does not disrupt the food supply (e.g., that stemming from agricultural or forestry residue as well that grown in nonarable land) is one of the few available resources with the potential to meet these challenges.

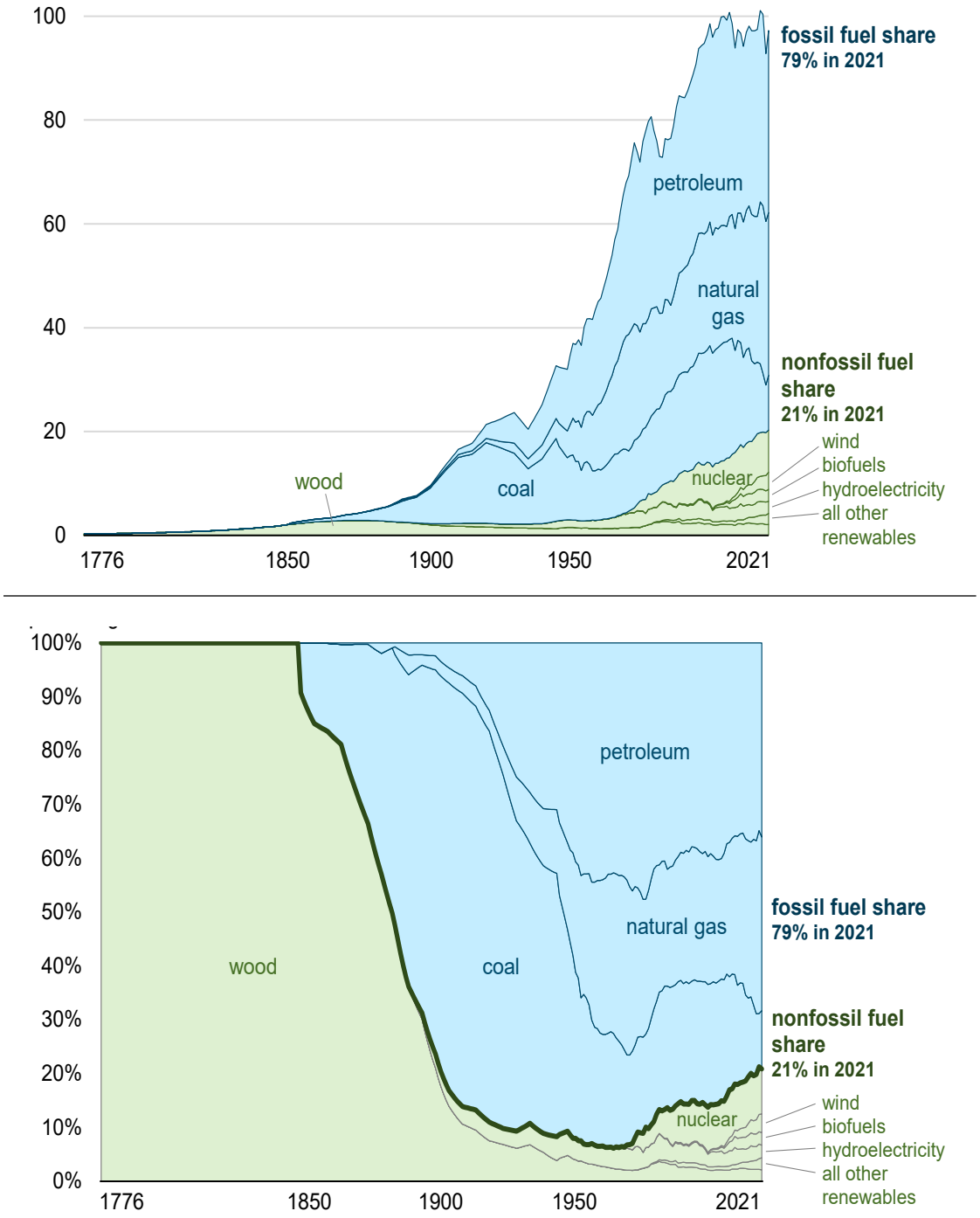

Figure 1.1. Annual energy consumption in the United States by major source (1776-2021) in quadrillion British thermal units (top), and as a percentage of total energy consumption (bottom). *Data Source:* U.S. Energy Information Administration, *Monthly Energy Review*.

Prior to the middle of the nineteenth century, biomass (in the form of wood) was the primary source of energy for heating, cooking, and lighting in the U.S. (Figure 1.1). Population growth necessitated a more efficient energy source in order to maintain the modern economy. Thus, for the better part of a century, the industrialized world has enjoyed abundant, inexpensive energy due to its reliance on fossil fuels. The widespread availability of inexpensive fossil fuels contributed significantly to the 20th century's rapid economic growth, which helped earn it the moniker "Petroleum Century" (Crocker 2010). The rapid economic growth of the industrialized world is largely attributable to the widespread use of petroleum, which has led to an increase in national and individual vehicle ownership. The increasing number of individuals with access to automobiles has increased the demand for liquid fuels. As a result, the U.S. shifted its focus from primary to secondary production, relying more and more on fuel imports from petroleum-rich regions such as South America and the Middle East. Consequently, the second half of the twentieth century witnessed a gradual transition from independence to dependence on foreign oil.

Most of the petroleum consumption in the U.S. stems from the transportation industry. In response to the increasing global demand for liquid transportation fuels, the production capacity of conventional petroleum reservoirs is rapidly contracting, exerting upward pressure on the global price of petroleum. In response to rising price volatility and supply unpredictability, a number of countries have enacted policies to increase domestic fuel production. In an effort to meet the rising demand for liquid transportation fuels, these initiatives frequently prioritize the utilization of biomass resources.

For example, in 2007, the U.S. government enacted the Energy Independence and Security Act (EISA) to reduce the nation's reliance on foreign oil and improve automobile fuel efficiency. Bioenergy (biomass-derived energy) has been identified as the most promising renewable resource for assisting the U.S. in achieving energy independence. The development of affordable domestic fuels and co-products, the reduction of greenhouse gas emissions, and the creation of domestic jobs to support the growth of the U.S. bioeconomy are all ways in which bioenergy can contribute to an economically sound and environmentally sustainable future. This is because bioenergy is a renewable resource that can be used to produce a wide range of products, including transportation fuels, thermal energy, electrical power, and platform chemicals typically derived from petroleum.

Biomass – i.e., all material of recent biological origin (such as plant or algal material, or animal waste) – is by its very nature a renewable feedstock. Processes capable of converting renewable biomass into fuels, chemicals, and bioproducts could reduce our reliance on nonrenewable fossil fuels and usher in a more sustainable bioeconomy. Theoretically, biofuels can be derived from carbon-neutral sources and drop-in biofuels can be easily integrated into existing vehicle fueling systems. The most common biofuels are liquid transportation fuels (and fuel blend stock) derived from these feedstocks (Crocker 2010). Utilization of biofuels in the U.S. dates to the 1970s, when they were introduced as a hedge against catastrophic supply disruptions caused by America's heavy reliance on imported oil (Tyner and Taheripour 2014; Jacobs 2016). Both ethanol and biodiesel, which were developed using first-generation biofuel technology (i.e., that using edible feedstock and/or affording biofuels that are not entirely fungible with fossil fuels), are the most popular biofuels today.

Indeed, ethanol, an alcohol derived from biomass that is used to increase the octane rating of gasoline and reduce emissions of carbon monoxide and other smog-causing pollutants, accounts for the vast majority of biofuel production in the U.S. Producing bioethanol from corn starch has been the most technologically advanced method for achieving this goal to date. Most of the ethanol used as a transportation fuel in the U.S. is produced domestically, which also produces the most ethanol of any country. A little more than 10 percent of all gasoline sold in the U.S. contains ethanol.

The U.S. Environmental Protection Agency (EPA) has set a target that by 2022, 36 billion gallons of gasoline will be produced from advanced biofuels other than cornstarch. This target was mainly set to prevent the production of biofuels from displacing agricultural land used for food production. There is substantial potential for lignocellulosic biomass as a feedstock for second generation biofuels (i.e., those produced using inedible feedstock and/or entirely fungible with fossil fuels), mainly because inedible biomass feedstocks are as diverse as they are abundant. For instance, due to their high polysaccharide content, starches can be easily converted into sugars, making them a most promising feedstock for biofuel production. Their low cost, high availability, also make them one of the most accessible renewable carbon sources. Cellulose, hemicellulose, and lignin make up the majority of lignocellulosic biomass, which can be derived from a vast array of materials, including food, crop, and wood residues; forest products and residues; as well as fast-growing, energy-specific crops (perennial grasses and woody crops) (Huber, Iborra, and Corma 2006). It is anticipated that the U.S. should have access to over one billion dry tons of lignocellulosic feedstocks by 2030 (Langholtz 2016).

The United States has high hopes for a transition to renewable fuels in the future, but there are many challenges that must be overcome before this can happen.

1.2 Lignocellulosic biomass conversion

At the industrial scale, biomass conversion takes place in facilities called biorefineries due to their similarities with petroleum refineries. Indeed, just as the latter do with petroleum, in biorefineries processes break down biomass raw materials and convert them to biofuels and bioproducts. In the same way that traditional refineries produce multiple streams of valuable products from petroleum (and do so in the most efficient and economical way possible), a biorefinery uses biomass as the feedstock (instead of petroleum) to produce materials, chemicals, fuels, and generate power efficiently, economically, sustainably (Hingsamer and Jungmeier 2019; Fernando et al. 2006). In a typical lignocellulosic biorefinery, plant material is physically processed before being chemically segregated via chemical digestion or enzymatic hydrolysis into three fractions: cellulose, hemicellulose, and lignin. The carbohydrate-based components (cellulose and hemicellulose) of lignocellulose can be used to commercially produce ethanol through fermentation (Abo et al. 2019). However, lignin valorization commercial processes are in earlier stages of development, so lignin is typically only used as a low-grade fuel to satisfy internal energy needs (Schutyser et al. 2017). Still, cellulosic ethanol biorefineries yield around 60% more lignin than is required to meet internal energy demands through its combustion (Ragauskas et al. 2014).

Before a biorefinery can begin commercial operations, techno-economic analyses must be performed to mitigate risk. Several studies have found that valorizing lignin – a highly aromatic natural phenolic polymer accounting for 15-30% of lignocellulose biomass by weight – has the potential to considerably contribute to the economic viability of biofuels (Schutyser et al. 2017; Davis et al. 2016). Notably, the National Renewable Energy Laboratory (NREL) stated in 2018 that lignin valorization was required to meet the target cost of $2.50/gal of gas equivalent from lignocellulose biomass (Davis et al. 2018). Similarly, Kautto et al. (2014) modeled a process for producing ethanol from hardwood, with lignin, furfural, and acetic acid as co-products. The value of the lignin co-product – as was also the case in the NREL findings – was a substantial factor in the calculation of the minimum ethanol selling price. Nevertheless, the value of lignin is currently limited by its resistance to chemical and biological manipulation, as well as a lack of cost-effective depolymerization techniques for converting it to valuable bioproducts (Alonso, Wettstein, and Dumesic 2012). Therefore, despite the fact that cellulosic ethanol can improve the economics of ethanol production because the feedstocks employed are mostly waste – e.g., byproducts of another industry (wood, crop residues) or specialized crops with lower water and fertilizer requirements than corn (Rosenfeld 2018) – the technology required to manufacture cellulosic ethanol has not advanced quickly enough to meet the EISA volume standards (Figure 1.2) due to the complexity and cost of depolymerizing lignin (Hanson 2018).

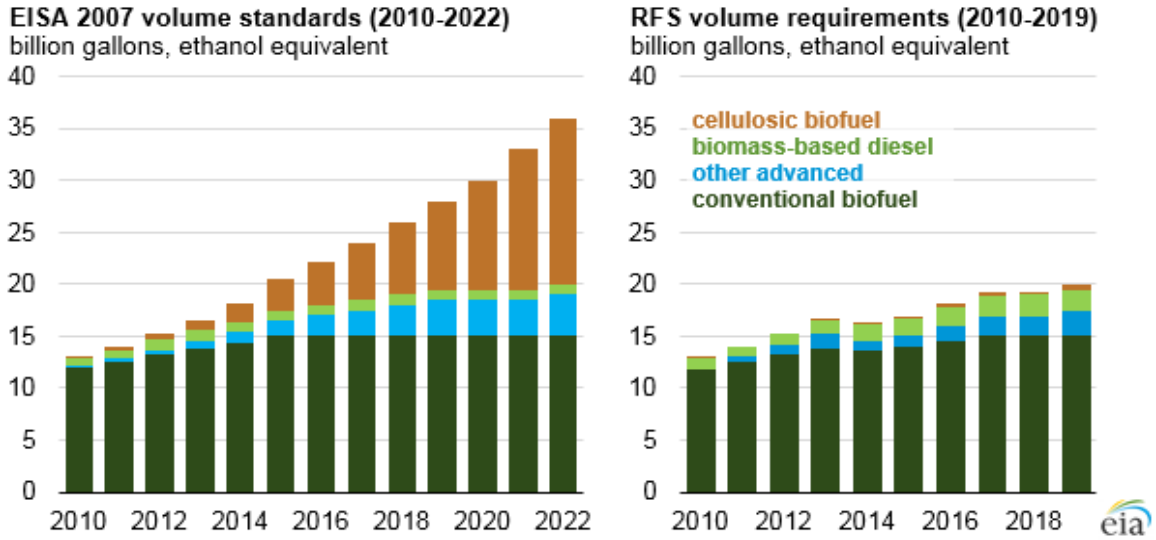

Figure 1.2. Volume standards (billion gallon, ethanol equivalent) as set forth in The Energy Independence and Security Act of 2007 (EISA).

1.3 Aim, objectives, and outline of this thesis

The overarching goal of the work described in this thesis focuses on the development of methods for the depolymerization of native lignin (lignin contained in lignocellulose), this being one of the main constituents of biomass. In doing so, this work aims to convert this largely waste material into a sustainable source of valuable chemicals and fuels, thereby significantly improving the economics of biorefineries.

Chapter Two discusses the structure and chemistry of lignin and illustrates the differences associated with lignin from various sources. A comprehensive overview of reductive catalytic conversion methods is also provided to familiarize the reader to the number of processing variables involved in the depolymerization of lignin with heterogeneous catalysts. Chapter 2 will also provide the groundwork for the following research objectives:

1. Evaluation of mono- and bi-metallic Ni-based catalysts supported on alumina to identify an effective formulation for reductive lignin depolymerization in sub- and supercritical methanol of a model soft wood (hybrid poplar).
2. Identification of the structure-activity relationships underpinning the performance of these catalysts at specified conditions via in-depth catalyst characterization.

In order to carry out these objectives, several tasks needed to be accomplished. These specific tasks include:

1. Catalyst preparation and characterization. Three different catalyst systems were investigated: (i) Monometallic Ni supported on alumina (20 wt.% Ni/Al_2O_3), (ii) Ni-Cu (20 wt.% Ni-5 wt.% Cu/Al_2O_3), (iii) Ni-Fe (20 wt.% Ni-5 wt.% Fe/Al_2O_3).
2. Catalyst activity evaluation for reductive catalytic fractionation (RCF). The efficacy of the catalytic treatments was assessed, based on characterization of the initial feedstocks and the resulting organic soluble oils, and recovered solids through GC-MS and elemental analysis. The goal of this task was to achieve a low molecular weight oil product with a high selectivity to monophenolic products.

The specific methodology and materials employed to perform the work described in this thesis are detailed in Chapter 3, while Chapter 4 is devoted to the presentation and discussion of the results obtained from and the fundamental insights gained from examining three important performance factors, the effectiveness of lignin extraction as measured by lignin oil production, the quantity and distribution of identifiable monomers in lignin oil, and the yield of residual solids following depolymerization experiments. Chapter 5 details the conclusions and recommendations for additional research on this subject.

CHAPTER 2. LITERATURE REVIEW

2.1 Introduction

The demand for renewable energy and alternatives to petroleum has increased in recent years due to environmental concerns and dwindling petroleum supplies. Biomass is an ideal source of the carbon, oxygen, and hydrogen needed to produce carbon-based goods and chemicals. The efficient transformation of lignin into monophenols is now the focus of many research efforts. This is because depolymerization can convert lignin, a highly aromatic and underutilized component of lignocellulosic biomass, into bulk quantities of aromatic compounds. These molecules provide a carbon-neutral, direct replacement for petroleum products, solving a number of problems at once.

In the presence of a heterogeneous catalyst, these aromatic compounds can be produced through either the oxidative or reductive depolymerization of lignin. Lignin depolymerization via selective oxidation requires high-priced catalysts and isolated lignin to produce monophenols. In order to circumvent the low product selectivity that comes from harsh isolation techniques, this research focuses on reductive methods that make full use of the biomass substrate without any prior processing. In this regard, reductive catalytic fractionation (RCF) is an attractive method since it makes use of moderate reaction conditions to enable more specific bond breaking in lignin.

Numerous authors have investigated the use of carbon supported monometallic Pd, Rh, Ru, or Ni catalysts for RCF (Renders et al. 2018; Renders et al. 2016; Schutyser et al. 2015; Van Aelst et al. 2020; Van Den Bosch, Schutyser, Koelewijn, et al. 2015; Van den Bosch, Schutyser, Vanholme, et al. 2015); however, the high cost and/or low stability of these catalysts may prevent their widespread commercial application. In recent years, it has become clear that Ni catalysts with added Cu or Fe can achieve the same levels of hydroprocessing activity as more expensive precious metal catalysts (Loe et al. 2019; Loe et al. 2016; Santillan-Jimenez et al. 2018). The goal of this study is to use secondary promoter metals like Cu and Fe to boost the activity and selectivity of Ni-based-alumina catalysts for depolymerizing native lignin via RCF. This review gives a comprehensive overview of reductive catalytic conversion methods to familiarize the reader with the many processing aspects that contribute to efficiently depolymerizing lignin in the presence of Ni-based heterogeneous catalysts. Since the structural properties of lignocellulosic biomass and lignin chemistry provide the foundation for fractionation and depolymerization techniques, they are briefly introduced at the outset.

2.2 Structural characteristics of lignocellulosic biomass

Lignocellulosic biomass, which makes up approximately 60-90 wt.% of terrestrial biomass, is composed of three major chemical fractions – cellulose, hemicellulose, and lignin – that vary significantly across grasses, softwoods, and hardwoods (Table 2.1).

Table 2.1. Distribution of common constituent fractions in lignocellulosic biomass types*

Biomass	Cellulose	Hemicellulose	Lignin	Other**
Hardwoods	46%	29%	22%	3%
Softwoods	41%	30%	27%	2%
Grasses	35%	17%	23%	22%

*Adapted from (Morton 2010); **Pectin, starch, ash, etc.

The structure of both lignocellulosic biomass and its compositional fractions are illustrated in Figure 2.1. Cellulose is a crystalline linear polysaccharide comprised only of D-glucose monomers linked by β-1,4 glycosidic linkages. It is the most prevalent terrestrial source of renewable carbon. Cellulose is typically composed of 5,000 to 10,000 D-glucose units that form a rigid, flat network by intra- and intermolecular H-bonding involving its hydroxy groups. As a result of these bonds, cellulose fibers have a high tensile strength and a tendency to be insoluble in the majority of solvents, including water (Huber, Iborra, and Corma 2006; Crocker 2010; Schutyser et al. 2018; Schutyser et al. 2017; Zakzeski et al. 2010).

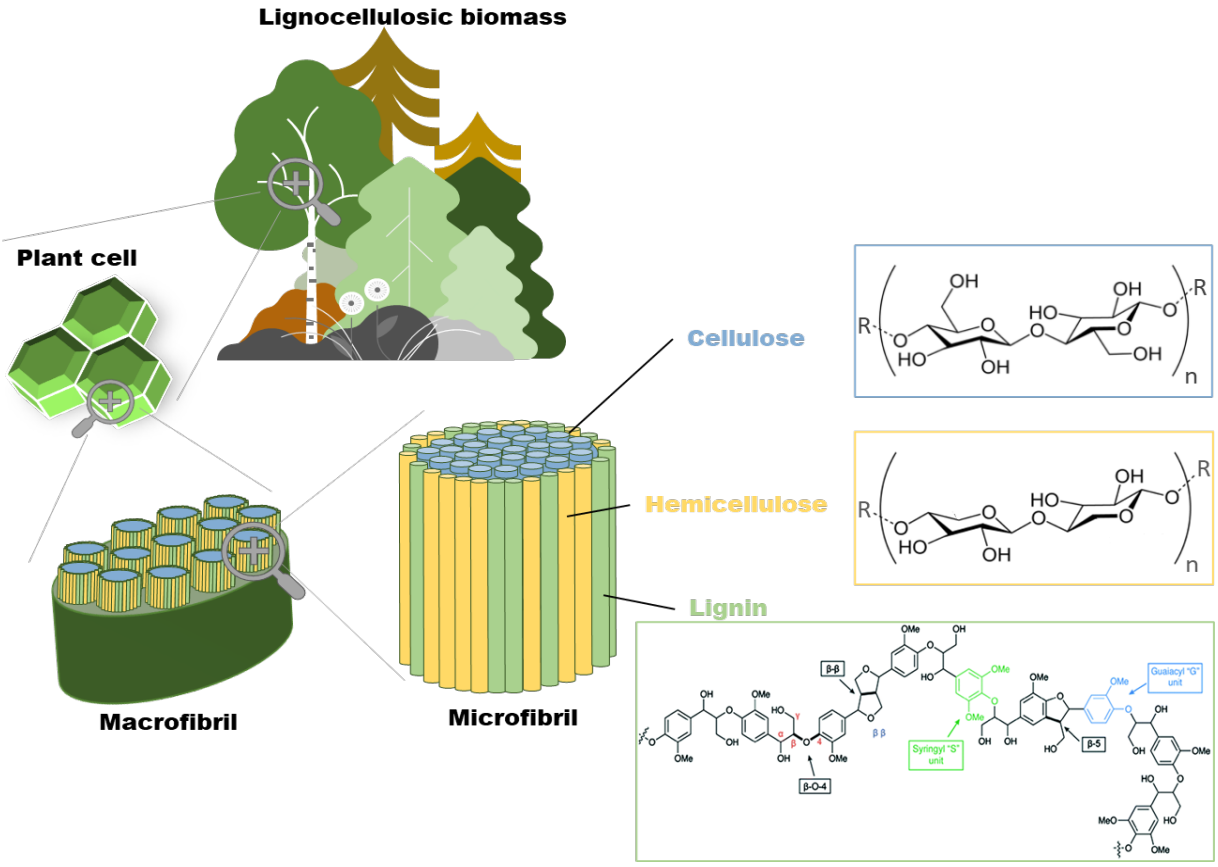

Figure 2.1. Schematic representation of lignocellulosic biomass structure and its constituent fractions.

Hemicellulose is a complex amorphous polymer made up of around 150 monomer units of hexoses (glucose, galactose, and mannose) and pentoses (xylose and arabinose) that form short, branched chain of polysaccharides that interact with cellulose and lignin to produce cell wall strength. Due to the presence of acetyl groups and its highly branched structure, it lacks the crystalline structure of cellulose and depolymerizes more readily (Huber, Iborra, and Corma 2006; Crocker 2010; Schutyser et al. 2018; Schutyser et al. 2017; Zakzeski et al. 2010).

In contrast to cellulose and hemicellulose, which are composed of simple sugars (monosaccharides), lignin is an amorphous 3-D polyphenolic compound that binds the entire network together. Lignin comprises 15-30% of lignocellulose by weight and resides in the cell wall by covalently linking with hemicellulose interlaced between cellulose microfibrils (Figure 2.1). Lignin's dense cross-linking provides the cell wall its structural integrity in addition to its ability to defend against chemical or microbial attack, all while facilitating water transport. Lignin is highly aromatic and therefore the most abundant renewable source of aromatic compounds on the planet, making it a possible replacement feedstock for petroleum-based chemicals if it can be effectively depolymerized into useable monophenols. However, the likelihood for secondary reactions to occur during depolymerization poses a significant challenge to lignin depolymerization processes (Huber, Iborra, and Corma 2006; Crocker 2010; Schutyser et al. 2018; Schutyser et al. 2017; Zakzeski et al. 2010).

2.3 Structure of lignin

Native lignin refers to lignin that resides within the lignocellulose substrate (Schutyser et al. 2018), which is made up of a complicated matrix of linkages that are formed through oxidative radical coupling of three primary monomer units (henceforth referred to as monolignols) in the cell wall. These monolignols are distinguished by the number of methoxy groups they contain, the presence of zero methoxy groups denoting the p-Coumaryl unit, one group denoting the Guaiacyl unit, and two groups denoting the Syringyl unit – abbreviated as H, G, and S units, respectively (Schutyser et al. 2018) (Figure 2.2). During radical coupling, the monolignols are joined via multiple random C-O and C-C interunit bonds, resulting in lignin's diverse structural units. β-O-4 bonds are the most prevalent and easiest to break during depolymerization, whereas β-5, β-β, 5-5, and β-1 bonds are more resistant to chemical degradation.

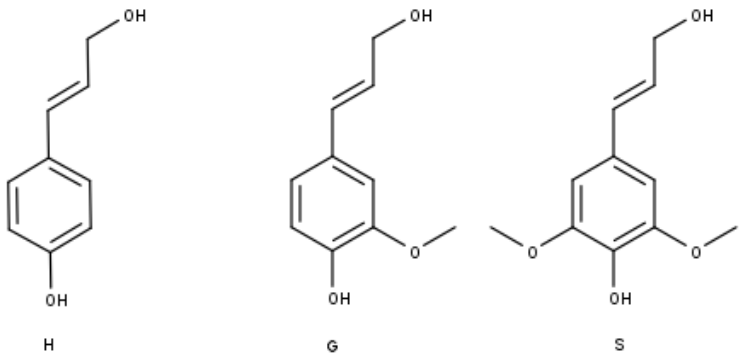

Figure 2.2. Primary monolignols for the formation of lignin. (H) p-Coumaryl alcohol; (G) Coniferyl alcohol; (S) Sinapyl alcohol.

The relative distribution of monolignols and subsequent formation of interunit bonds varies significantly between lignin sources (Table 2.2). For example, softwoods such as pine are almost entirely composed of G units, whereas hardwoods (e.g., birch, poplar) are composed of both G and S units. Perennial grasses and fibrous biomasses like switch grass and corn stover typically contain low concentrations of all three units (Schutyser et al. 2018).

Table 2.2. Bonding motifs and potential targets for lignin depolymerization with relative percentages by biomass type.*

Biomass type	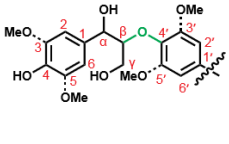 β-O-4	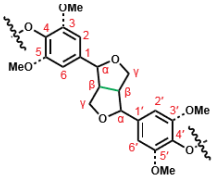 β-β	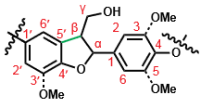 β-5	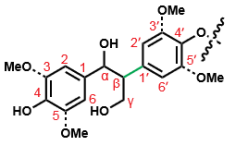 β-1**
Softwood	45-50%	9-12%	2-6%	1-9%
Hardwood	60-62%	3-11%	3-12%	1-7%
Grasses	74-84%	5-11%	1-7%	n.d.%

*Percent occurrence values reported in recent review by Rinaldi et al. (2016); **β-1 moieties exist in lignin as a spirodienone structure are converted to the β-1 structure shown after ring opening under mildly acidic conditions (Rinaldi et al. 2016; Zhang and Gellerstedt 2001).

In addition to the major monolignols outlined above, significant concentrations of p-hydroxybenzoate (0.5 to 3.0 wt.% of lignin) are contained in all poplar hardwood species (Goacher, Mottiar, and Mansfield 2021; Smith 1955). During hydrogenolysis reactions, this lignin-bound p-hydroxybenzoate is liberated by transesterification to generate p-hydroxybenzoic acid methyl ester (denoted as MP/pHBA throughout this thesis) (Schutyser et al. 2018).

The "S/G ratio," or relative amount of S and G in lignin, is a metric used to represent the abundance of β-O-4 linkages in the matrix because the presence of easily cleavable bonds, like β-O-4, makes lignin removal and degradation easier. These monolignols are the key to the conversion of lignin to platform chemicals because the fragmentation of their linkages leads to the formation of simpler compounds that resemble H, G, and S units. Indeed, it is precisely the structural robustness and complex structure of lignin makes the lignocellulose recalcitrant to chemical degradation or conversion to useful products. The formation of refractory bonds is defined as the recalcitrance whereby the physiochemical, structural, and compositional factors of lignocellulose hinder the direct chemical or biological deconstruction of cellulose (Schutyser et al. 2017). In other words, to gain access to the valuable cellulose fraction – resulting in ethanol from the conversion of glucose – the lignin must first be removed from the matrix.

2.4 Lignin depolymerization

Heterogeneous catalytic processes for depolymerizing lignin are often carried out with the help of catalysts based on noble metals. Transition metals like nickel, iron, and copper are also commonly studied, but palladium, ruthenium, and rhodium are far more commonly employed as catalysts due to their high activity. Catalysts comprising more than one metal – as an alloy and/or as a combination of metal and metal promoter(s) – are widely used in the field of catalysis as these formulations often afford better and more tunable results relative to monometallic catalysts (Sharma et al. 2017).

The presence of more than one metal offers a different surface electronic environment and geometric structure relative to a single metal, which confers on multimetallic catalysts unique electronic and chemical properties that can result in improved activity, selectivity, and/or stability (Yu, Porosoff, and Chen 2012). It is thus unsurprising that multimetallic formulations are commonly used – and often preferred – to catalyze reactions as numerous as they are varied, including hydrogenation, dehydrogenation, reduction, oxidation, water gas shift (WGS), and reforming, the use of multimetallic formulations for biomass upgrading being particularly noteworthy (Sankar et al. 2012; Alonso, Wettstein, and Dumesic 2012).

The lignin structure is altered by various de- and re-polymerization reactions in any strategy for biomass or lignin processing. The formation of monomeric aromatic compounds from lignin depolymerization results in hydroxyl, allylic alcohol, aldehyde, ether, or carboxylic acid substituents depending on the processing method employed (Jongerius 2013). Thus, selective depolymerization of lignin utilizing heterogeneous catalysts can afford aromatic monomers commonly derived from the petroleum industry and used to produce the chemicals and materials that enable modern society (Figure 2.3).

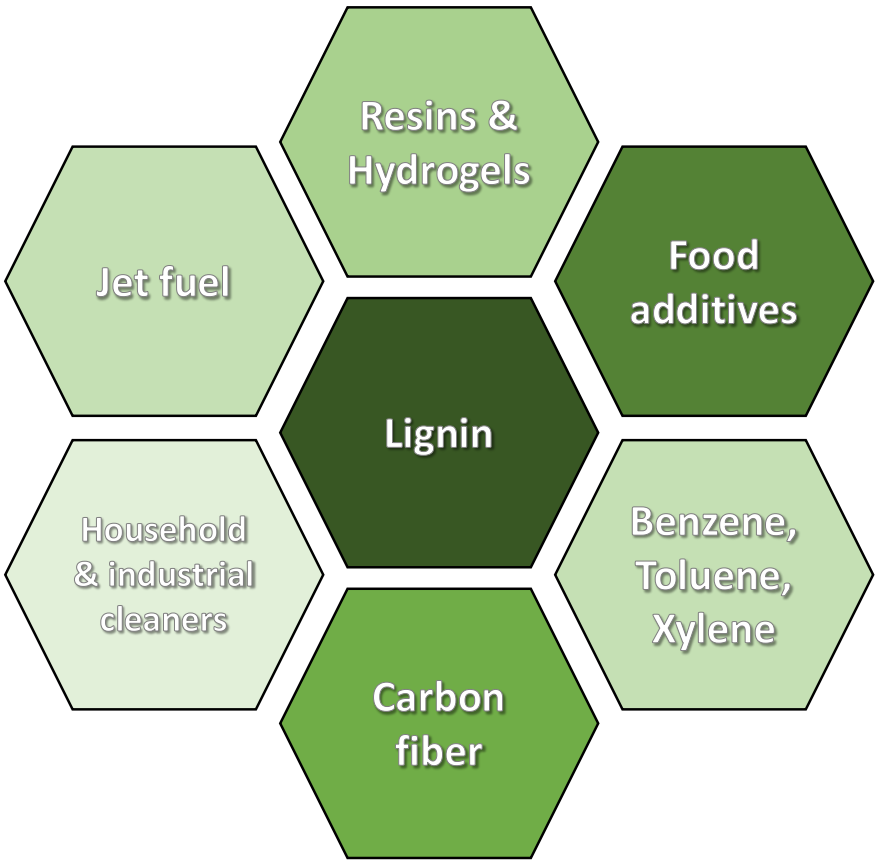

Figure 2.3. Value-added products from lignin feedstocks (Gale, Cai, and Gilliard-Abdul-Aziz 2020; Johnson 2007).

When utilizing heterogeneous catalysts, the depolymerization of lignin occurs in the presence of either oxidative or reductive conditions. Although the oxidative route can result in highly functionalized, and therefore valuable, aromatic compounds such as vanillin, an extensively utilized flavoring agent in the food industry and a chemical intermediate in pharmaceutical manufacturing (Jenkins and Erraguntla 2014). Parenthetically, the market for vanillin is too small to accommodate for the large quantity of isolated lignin produced during biomass processing. Additionally, lignin depolymerization by selective oxidation requires isolated lignin as the feedstock, so lignin recalcitrance due to refractory C-C bond formation is unavoidable.

In contrast, hydroprocessing techniques – reductive approaches that utilize hydrogen to thermochemically reduce the feedstock – continue to be among the most prevalent and efficient methods for depolymerizing lignin into smaller molecules (such as low molecular weight lignin, phenols, and other useful chemicals) and to convert those molecules into hydrocarbon fuels (Shen et al. 2016; Gale, Cai, and Gilliard-Abdul-Aziz 2020).

Hydrogenolysis – the scission of chemical bonds (like C-C or C-O bonds) via hydrogen addition – has become one of the most widely used and effective lignin depolymerization procedures to produce aromatic compounds and facilitate C-O bond breaking (primarily interunit β-O-4 linkages) (Shen et al. 2016). This reaction can occur in the absence of catalysts; however, catalysts can help employ H_2 to selectively break certain bonds. Hydrodeoxygenation (HDO) is a kind of hydrogenolysis in which C-O bonds are broken and oxygen is eliminated as H_2O. HDO is frequently utilized to remove unwanted oxygen from the lignin fraction. The presence of oxygen in the structure of lignin and its derivatives restricts their use in fuels and chemicals due to the lowering of heating value and energy density. Excessive oxygen can also result in high acidity and reactivity, which complicates the storage of biomass and reduces its shelf life. Realization of biorefinery schemes with fully integrated lignin valorization processes requires the development of catalytic technology for lignin depolymerization.

In short, the inefficient depolymerization of lignin is a major impediment to the development of a sustainable bioprocessing sector utilizing lignocellulosic biomass. However, the current catalysts systems in the petroleum industry are not fit for this purpose. The latter is not surprising, since biomass consists of oxygen-rich long-chain molecules, whereas the long chain hydrocarbon molecules constituting petroleum are oxygen-poor (Alonso, Wettstein, and Dumesic 2012).

2.5 Catalytic upgrading of lignin

In the 1940s, high pressure hydrogenolysis/hydrogenation of wood was first used to elucidate the structure of native lignin (Song 2019). Maple, aspen, and spruce, were hydrogenated in a 1:1 dioxane/water solvent mixture under various process conditions (173-220 °C, 35-210 bar H_2, 5-6 hours) using Raney Ni, a finely powdered Ni-based solid (Pepper and Hibbert 1948; Pepper and Lee 1970; Pepper and Steck 1963). In the past decades, lignin depolymerization has expanded to encompass a wide variety of methods. Schutyser et al. (2018) have provided a comprehensive description of lignin depolymerization strategies.

Briefly, the reductive cleavage of lignin can be separated into two main strategies, namely, early stage (i.e., lignin-first) and late stage, with the main difference being when lignin is extracted from the lignocellulose matrix. In late stage reductive depolymerization, lignin is extracted from lignocellulose using isolation techniques such as alkaline pulping, organosolv processing, enzymatic processing, and mild acidolysis. These pretreatment methods can render lignin more difficult to valorize due to the formation of new refractory bonds that form during the isolation process.

On the other hand, early stage, commonly referred to as reductive catalytic fractionation (RCF), utilizes lignin that is removed from the cell wall during hydrogenolysis using heat and solvents, usually in the presence of a catalyst (Renders et al. 2019). The lignin is immediately depolymerized with negligible condensation, thus circumventing additional recalcitrance, leading to higher product yields relative to technical lignin. This 'lignin-first' approach can be advanced by utilizing active and selective heterogenous catalysts to maximize yields, minimize residues, decrease environmental impact of chemical processes, and produce products at low prices so these products can be competitive in the current market.

2.6 Reductive Catalytic Fractionation (RCF)

The most common methodology for RCF involves the solvent-based extraction of lignin from biomass in the presence of a transition metal under hydrogen atmosphere, with the aid of an H-donor solvent, or with another reducing agent (Ferrini and Rinaldi 2014; Parsell et al. 2015; Song et al. 2013; Van den Bosch, Schutyser, Vanholme, et al. 2015; Yan et al. 2008). The technical distinction of RCF is the utilization of a heterogenous catalyst, whose primary role involves the reductive stabilization of reactive intermediates that result from the solvolysis of lignin, and the depolymerization of the solubilized oligomers produced (Abu-Omar et al. 2021). Although numerous attempts have been made to improve the efficiency of the RCF process using catalysts, the latter is still insufficient for widespread industrial application (Bartling et al. 2021).

The development of heterogeneous catalysts for RCF is heavily reliant on an understanding of material design concepts related to the way in which the metal(s) and the support comprising the catalyst – as well as the solvent employed – can improve selectivity and conversion (Gale, Cai, and Gilliard-Abdul-Aziz 2020). To maintain aromaticity, optimal catalyst features for reduction reactions include: (1) high conversion at low temperatures to minimize char formation and competitive thermal condensation reactions; (2) high selectivity to phenols to avoid excessive hydrogen consumption; (3) water tolerance; and (4) the ability to deal with a variety of lignin streams (Zakzeski et al. 2010). These characteristics stem from the fact that the RCF process is influenced by three major factors: (1) feedstock; (2) solvent/H-donor system; and (3) catalyst type (Renders et al. 2017).

2.6.1 Lignin feedstock

The variability of lignin structure and cross condensation reactions contribute to the difficulty of biomass processing by affecting yields. Therefore, conventional biorefinery schemes, such as those used in the pulp and paper industry, employ pretreatment processes to remove lignin from the lignocellulose matrix as a waste material to be burned for internal heat and power (Gale, Cai, and Gilliard-Abdul-Aziz 2020; Schutyser et al. 2018). To separate the insoluble cellulose fibers from the soluble lignin, a technique is used to solubilize the lignin fraction, and the resulting byproduct is called "technical lignin." Lignin is often extracted using either sulfur-based technologies, such as sulfites affording Kraft lignin, or sulfur-free procedures, in which organic solvents or alkaline solutions are utilized.

The most common types of technical lignins are lignosulphonates (obtained via sulfite pulping), Kraft lignins (obtained via Kraft pulping black liquor), organosolv lignins (obtained via organosolv pulping), soda lignins (obtained via soda pulping), and lignin residue after enzymatic treatment of biomass (Bulkowska 2016). Removing the lignin in this way yields a very concentrated form of lignin that is mostly made up of refractory C-C bonds. Although the pulp and paper industry produce nearly 70 Mt of technical lignin annually, only a small fraction of this technical lignin – primarily lignosulfonates (derived from sulfite processing) – are utilized commercially as binding and dispersing products; the rest is combusted as low-grade fuel for internal heat and power (Ragauskas et al. 2014).

Technical lignin is typically recalcitrant to depolymerization to monophenols because it lacks easily cleavable C-O linkages, requiring harsher process conditions to break C-C bonds instead. For example, Narani et al. (2015) depolymerized Kraft lignin to alkylphenolics using supported NiW and NiMo catalysts in supercritical methanol (T: 320 °C; p: 35 bar H_2, t: 8 hours) resulting in 26 wt.% of alkylphenolics. These authors concluded that the high sulfur content of Kraft lignin may lead to catalyst deactivation. Similarly, Dou et al. (2021) depolymerized Kraft lignin over a hollow Ni-Fe catalyst in a methanol/1,4-dioxane mixture (T: 300 °C; p: 20 bar H_2, t: 3 hours) resulting in a maximum of 70 wt.% of monomers and dimers. In doing so, these authors demonstrated that the efficient conversion of Kraft lignin into alkylphenols under mild conditions requires the synergetic effects of multimetallic catalysts to circumvent the catalyst deactivation resulting from the use of less-than-ideal feedstocks like technical lignin.

Due to the complicated physiological properties of lignocellulosic biomass, the use of bimetallic Ni-based catalysts for the conversion of native lignin is still relatively underexplored, despite the widespread recognition of the higher performance of multimetallic catalysts. Most studies begin with the catalytic conversion of lignin model compounds such as phenol, anisole, and guaiacol to better understand catalytic activity (Chen et al. 2019). For instance, an isopropanol-based solvent was used in the catalytic transfer hydrogenation of p-cresol by Kannapu et al. (2015), who used a bimetallic Ni-Cu/Al_2O_3 formulation. With the Ni-Cu/Al_2O_3 catalyst, a variety of products were obtained from the reduction of p-cresol in isopropanol at a yield of >95%, which confirms that Ni-Cu catalysts are effective for transfer hydrogenation of p-cresol and furfural.

2.6.2 Reaction conditions

The chemical make-up of aromatic product mixtures can be modified not only by varying or modifying the catalyst, but also by the altering the solvent and other process parameters like temperature and pressure. The solvent employed greatly influences the product distribution in lignin depolymerization. For example, basic solvents such as methanol reduce the catalytic activity for hydrogenation of aromatic products but do not affect the hydrogenolysis of ether bonds and improve the selectivity towards phenols (Shen et al. 2016). In addition, the degree of delignification, retention of (hemi-)cellulose as pulp, and selectivity to monophenolics are all impacted by the solvent system (Renders et al. 2017). Schutyser et al. (2015) investigated the role of various solvents as the determining factor for optimal conversion of wood for both high carbohydrate retention and efficient delignification.

In this study, a range of solvents were tested via RCF of birch sawdust in the presence of Pd/C catalyst at 200 °C under a hydrogen atmosphere for 3 hours. Close observation of solvent effects revealed a relationship between high polarity and increased delignification capability, with excessive polarity resulting in carbohydrate loss. To account for the products of conversion, an empirical descriptor was utilized to rank the solvents based on their process efficiency and the value for methanol was found to be 80% – the maximum value among the solvents tested. Renders et al. (2016) investigated the influence of alcohol and water on the RCF of poplar wood. In this study, 2 g of pre-extracted sawdust was reacted with 0.2 g of catalyst powder (Pd/C) in a range of solvent mixtures (40 mL) comprised of different volumetric ratios of MeOH/water or EtOH/water. The authors obtained higher product yields in lignin conversion while MeOH and EtOH were mixed with water compared to any one solvent used on its own, MeOH and EtOH displaying very similar maximal degrees of delignification for water concentrations between 30 and 70 vol.%. At mild temperatures, the addition of water to an alcohol solvent significantly enhanced lignin extraction, due to the polarity of the mixture. Van den Bosch et al. (2017) analyzed the RCF process in detail to investigate the specific roles of catalyst and solvent to determine the potential of commercial Ni/Al_2O_3 pellets. In this study, the authors performed reactions on birch sawdust and in methanol focusing on a range of ways to incorporate the Ni/Al_2O_3 catalyst (i.e., in a basket, mixed with solvent, pelletized, or as a fine powder). Van den Bosch and co-workers observed that the presence of the Ni/Al_2O_3 catalyst only slightly increased the rate of bond cleavage, which proceeded via solvolysis. Under the applied conditions it was unambiguously demonstrated that the solvent was entirely responsible for the extraction of lignin.

2.6.3 Catalyst active phase

Typically, heterogeneous catalysts for reductive lignin depolymerization are composed of noble metals such as Pd (Kim et al. 2015; Schutyser et al. 2015; Parsell et al. 2015; Van Den Bosch, Schutyser, Koelewijn, et al. 2015; Renders et al. 2016), Ru (Anderson et al. 2016; Kim et al. 2015; Van den Bosch, Schutyser, Vanholme, et al. 2015; Liao et al. 2020), or Rh (Anderson et al. 2019; Liao et al. 2020). Albeit Ni-based catalysts exhibit lower reactivity they also display greater selectivity, particularly towards aromatic monomers (Chen et al. 2019). Notably, the operating costs of a biorefinery are extremely sensitive to the cost, stability, and reusability of the heterogeneous catalyst employed (Cooreman et al. 2020). Ni is currently priced ~96, ~15, and ~3 times less than Rh, Pd, and Ru, respectively (Els 2020). Utilizing noble metal catalysts supported on carbon has resulted in high monomer yields, but the price of the catalysts makes their use impractical.

Against this backdrop, several groups have used Ni-based catalysts for the reductive cleavage of native lignin. Indeed, the RCF of native lignin over Raney Ni (R-Ni) is detailed in Table 2.3. Abbreviations for primary monomers obtained can be found in Appendix A.

Table 2.3. RCF of native lignin over Raney Ni

Entry (#)	Feedstock	Catalyst	Solvent	T (°C)	p (bar)	t (h)	Primary monomers (wt.%)	Total monomer yield (wt.%)	Reference
1	Maple	R-Ni + NaOH	Dioxane/H_2O (1:1)	173	210 H_2	6	15% ES, 6% EohS	27	(Pepper and Hibbert 1948)
2	Aspen	R-Ni	Dioxane/H_2O (1:1)	220	35 H_2	5	29% PS, 13% PohS	59	(Pepper and Steck 1963)
3	Spruce	R-Ni	Dioxane/H_2O (1:1)	195	35 H_2	5	17% 4-propanolcyclohexanol	17	(Pepper and Lee 1970)
4	Poplar	R-Ni	2-PrOH/H_2O (7:3)	180	Auto	3	PohS	25	(Ferrini and Rinaldi 2014)
5	Poplar, spruce	R-Ni, Ni_2P/SiO_2	2-PrOH/H_2O (7:3)	180	Auto	3	50-60% phenolic species	20-25	(Cao et al. 2018)
6	Poplar, spruce	R-Ni	2-PrOH/H_2O (7:3)	200	Auto	6	NP	NP	(Graca et al. 2018)
7	Poplar	R-Ni	2-PrOH/H_2O (7:3)	200	Auto	3	11% PohS, 10% PohG	34	(Sultan et al. 2018)
8	Poplar, spruce	R-Ni	2-PrOH/H_2O (7:3)	220	Auto	3	10% ES, 7% PS	36	(Rinaldi et al. 2019)

*NP = not provided

Ferrini and Rinaldi (2014) explored a direct biorefining approach that focuses on producing low-molecular weight lignin intermediates. In this work, wood was "cook[ed]" in the presence of Raney Ni in 2-propanol (2-PrOH)/H_2O at various temperatures and timeframes (Table 2.3, Entry 4). The lignin in the wood was released as low molecular weight fragments, which were isolated in a non-pyrolytic lignin oil, alongside to pulps suitable for enzymatic hydrolysis. A suspension of wood pellets and Raney Ni catalyst in an aqueous solution of 2-propanol was heated (e.g., 180 °C) and mechanically stirred for 3 h to yield 25 wt.% lignin oil and 71 wt.% carbohydrate pulp. The lignocellulosic feed was processed without molecular hydrogen, and the acetone produced by hydrogen transfer can be hydrogenated to 2-PrOH. The holocellulose (cellulose and hemicellulose) fraction or pulp was separated and washed with a 2-PrOH/water solution, a magnet being used to remove Raney Ni from the suspension. As a final step, the solvent used to extract the non-pyrolytic lignin bio-oil was evaporated. The authors observed that the lignin had further depolymerized and had not repolymerized like it does in the industrial organosolv process, concluding that more research into catalytic biorefining methods has great potential for the production of alkanes or arenes. The complexity of the low-molecular weight lignin product mixture is a downside of this approach, although the use of autogenous hydrogen is advantageous. Cao et al. (2018) proposed an integrated biorefinery scheme, which involves producing gasoline and kerosene/diesel drop-in fuels in two phases (Table 2.3, Entry 5). In the first step, poplar and spruce were depolymerized over a Raney Ni catalyst in an isopropanol-water solvent mixture to yield lignin oils and cellulosic pulps. By adjusting the hydrogen pressure and temperature in the presence of a Ni_2P/SiO_2 catalyst, the lignin oils were converted to aliphatics or aromatics, respectively.

Hydrogen self-sufficiency was achieved by gasification of the delignified holocellulose fraction. The Rinaldi group defined the role of the Raney Ni catalyst in another paper as inhibiting formic acid synthesis via sugar hydrogenation (Graça et al. 2018) (Table 2.3, Entry 6). Rinaldi and colleagues also achieved proof-of-concept membrane filtration in 2019 for the separation and concentration of the monophenol-rich fraction from the lignin liquors (Sultan et al. 2019) (Table 2.3, Entry 7). The same group investigated the impact of reaction temperature in a subsequent article, using the same feedstock, catalyst, and solvent mixture (Table 2.3, Entry 8). Higher process temperatures resulted in higher overall delignification yields (up to 87%), low molar mass fragments, and preferential hydroxyl group cleavage in monolignol sidechains by hydrodeoxygenation, providing oils with decreased oxygen concentration (Rinaldi et al. 2019). Raney Ni is widely used in industry due to its high activity, low cost, and ease of separation; thus, its use in the catalytic conversion of biomass has garnered significant attention (Sun et al. 2021). However, since the catalyst has a large surface area and stores a large volume of hydrogen gas, it is extremely pyrophoric and must be handled with care and never exposed to air to prevent the production of toxic fumes, which has significant implications for process design and safety as well as operating costs.

Ni supported on a carbonaceous support (Ni/C) is also frequently investigated for reductive lignin depolymerization (Table 2.4). Li et al. (2012) investigated various feedstocks, solvents, and catalysts for reductive lignin depolymerization (Table 2.4, Entry 1). They found that hardwoods were converted into lignin and carbohydrates more efficiently than softwood. The monophenol yields increased when the original water solvent was replaced with methanol or with ethylene glycol.

In the presence of Ni-W_2C/C and ethylene glycol, the lignin component was selectively converted to monophenols with a yield of 47%. However, the best selectivity (56%) was obtained when a Pd/C catalyst was used. This process employed 60 bar of hydrogen gas. Song et al. (2013) investigated a fragmentation-hydrogenolysis approach for depolymerizing native lignin (Table 2.4, Entry 2). Pre-extracted birch sawdust was depolymerized in the presence of a Ni/C catalyst and several alcoholic solvents. Nuclear magnetic resonance (NMR) analysis revealed that lignin was fragmented into dimers and oligomers via solvolysis and further converted to monophenols by the Ni/C catalyst. The authors concluded that Ni-based catalysts are highly active and selective in native lignin conversion. Over a Ni/C catalyst in methanol, the influence of substrate and catalyst loading was studied (Table 2.4, Entry 3): birch resulted in higher monomer yields than poplar and eucalyptus, while higher catalyst loading resulted in higher monomer yields due to the presence of additional hydrogen generated from methanol reforming (Klein, Saha, and Abu-Omar 2015). Luo et al. (2016) investigated the effectiveness of Ni-based heterogenous catalysts in the catalytic depolymerization of lignin (CDL) (Table 2.4, Entry 4). In this study, miscanthus grass was reacted with 5-15 wt.% Ni/C catalysts in methanol at 225°C and 10-35 bar of H_2 for 12 hours. Using a 15 wt.% Ni/C catalyst, the three key components of miscanthus (lignin, cellulose, and hemicellulose) were efficiently transformed (55% overall conversion) into high value chemicals, with a 68% yield of phenolic compounds from lignin and a mass balance of 98%. Anderson et al. (2016) examined the RCF of corn stover in methanol at 200 and 250 °C using a Ni/C catalyst and H_3PO_4 as co-catalyst to gain insight into the solvolysis and fragment stabilization mechanisms of the system (Table 2.4, Entry 12). They found that RCF in the presence of supercritical methanol resulted in moderately higher

monomer yields with shorter reaction times relative to subcritical reactions at 200 °C. The total mass of lignin oil obtained was identical to that resulting from extractions in the presence of a metal catalyst, the direct solvolysis of lignin linkages being observed when operating without a reduction catalyst. The highest monomer yields were observed at 3 hours. There were clear trade-offs between lignin extraction levels, monomer yields, and carbohydrate retention in the recovered solids. The depolymerization of naturally occurring C-lignin, which consists only of caffeyl alcohol units, was investigated using RCF of vanilla seeds in the presence of Ni/C (Table 2.4, Entry 9). Only two products (propyl- and propenyl catechol) were obtained with a 21 wt.% lignin monomer yield (Stone et al. 2018). Poplar RCF catalyzed by Ni/C resulted in cellulose recalcitrance to enzymatic digestion (Table 2.4, Entry 11). Following gelatinization in trifluoroacetic acid, rates of enzymatic digestion or maleic acid/$AlCl_3$-catalyzed conversion to hydroxymethylfurfural (HMF) and levulinic acid (LA) were increased. These findings guided the development of a "no carbon left behind" strategy for converting total woody biomass into lignin, cellulose, and hemicellulose value streams for future biorefineries (Yang et al. 2019). Birch was effectively depolymerized in MeOH employing a Ni-Fe/C catalyst with an alloy structure (Table 2.4, Entry 6) yielding 40% monomer yield and 88% selectivity to 4-propylsyringol and 4-propylguaiacol (Zhai et al. 2017).

Table 2.4. RCF of native lignin over Ni-based catalysts

Entry (#)	Feedstock	Catalyst	Solvent	T (°C)	p (bar)	t (h)	Primary monomers (wt.%)	Total monomer yield (wt.%)	Reference
1	Birch	Ni-W_2C/C	Ethelyne glycol	235	60 H_2	4	18% PS, 10% PohS	47	(Li et al. 2012)
2	Birch	Ni/C	MeOH	200	1 Ar	6	36% PS, 12% PG	54	(Song et al. 2013)
3	Birch	Ni/C	MeOH	200	2 N_2	6	18% PS, 10% PG	32	(Klein, Saha, and Abu-Omar 2015)
4	Miscanthus	Ni/C	MeOH	225	60 H_2	12	19% PS, 21% PG	68	(Luo et al. 2016)
5	Beech	Ni/C	MeOH/H_2O (3:2)	200	60 H_2	5	29% PS, 10% PG	51	(Chen et al. 2016)
6	Birch	NiFe/C	MeOH	200	20 H_2	6	24% PS, 11% PG	40	(Zhai et al. 2017)
7	Poplar	Ni/C	MeOH	190	60 H_2	3	12% PG and PS	17	(Anderson et al. 2017)
8	Poplar	Ni/C	MeOH	200	30 H_2	1	8% PS, 5% PG	48	(Anderson et al. 2018)
9	Vanilla seeds	Ni/C	MeOH	250	30 H_2	3	18% propylcatechol, 3% propenylcatechol	21	(Stone et al. 2018)
10	Oak	Ni-Al_2O_3/AC	CH_2O_2/EtOH/H_2O	190	Auto	3	9% PS, 5% PG	23 C%*	(Park et al. 2019)
11	Poplar	Ni/C	MeOH	225	35 H_2	12	PS, PG	90	(Yang et al. 2019)
12	Corn stover	Ni/C	MeOH	250	30 H_2	3	7% methyl ferulate, 7% methyl coumarate	29	(Anderson et al. 2016)
13	Birch	Ni/Al_2O_3	MeOH	250	30 H_2	3	21% PohS, 5% PS	36	(Van den Bosch et al. 2017)

*C% = based on the percentage of C atoms present rather than wt.%

Although most of the catalytic lignin upgrading occurs in batch reactors, investigations of RCF in continuous systems are essential to inform realistic scale-up because they may offer time-resolved product distributions and yields. Anderson et al. (2017) published a report on RCF employing a flow-through system rather than a batch reactor (Table 2.4, Entry 7). These authors used two flow-through systems: a single-bed reactor with a biomass bed positioned upstream of a catalyst bed and a dual-bed reactor with switchable biomass beds physically isolated from the catalyst in a separate upstream reactor. In this study, RCF of poplar using a Ni/C catalyst in methanol solvent afforded a monomer yield of 17% (mostly propyl substituted guaiacol and syringol). Flow-through experiments, it was found, enabled the detection of biomass extraction intermediates, the decoupling of solvolysis and hydrogenolysis, simple catalyst recovery and recyclability, and the elucidation of catalyst deactivation mechanisms (Anderson et al. 2017). Anderson and co-workers continued to build continuous systems and conducted kinetic investigations of RCF in flow-through reactors, which indicated that the two limiting mechanistic stages, lignin solvolysis and reduction, can be regulated independently (Table 2.4, Entry 8). The difference in activation barriers between flow and batch reactors revealed that lignin extraction was mass transfer-limited under normal RCF conditions (Anderson et al. 2018). In another contribution (Table 2.4, Entry 10), formic acid was used as a hydrogen source and as a co-catalyst alongside Ni-Al_2O_3/AC, and a direct relationship was observed between spillover hydrogen on the catalysts and lignin-derived phenolic monomer yields (Park et al. 2019).

Although many of these publications highlight results near a theoretical yield (assuming only β-O-4 bonds are broken), the use of carbon-supported metal catalysts is undesirable since the regeneration catalyst deactivated through coking and fouling, is typically performed via the combustion of the carbonaceous deposits in hot air, which would inherently lead to the destruction of the catalyst support.

2.6.4 Catalyst support effects

The nature and roles of the carrier employed to prepare supported metal catalysts are crucial. Catalytic activity is intrinsic to the atomic layers constituting the surface of the catalyst. To preserve the surface area and thus the activity of the catalyst for a longer period, metals and oxides are typically deposited onto a thermally stable support that keeps active particles separated (Bowker 1998). Additionally, the support can impact the catalytic activity via steric and/or electronic effects. Activated carbon (AC) is one of the most common supports for biomass upgrading due to its high surface area and microporosity. Favorable characteristics in other common supports – including metal oxides such as alumina (Al_2O_3) – are the presence of mesopores, high thermal stability, and ability to be shaped into different structures. Oxidic supports, which are easily recyclable, are the more practical option for widespread industrial application (especially since they facilitate coke removal). The Lewis acid sites in the alumina support have also been found to play a significant role in the depolymerization of lignin, leading to an increase in the amount of low molecular weight compounds produced (Gale, Cai, and Gilliard-Abdul-Aziz 2020; Shen et al. 2016). Solubilization, depolymerization, and stabilization of birch lignin in methanol by a Ni/Al_2O_3-catalyzed system were determined to be catalyzed by hydrogenation of reactive intermediates,

whereas the solvent was revealed to be responsible for the first two steps. A catalyst basket aided in the recovery and reuse of the Ni/Al_2O_3 pellets, which were easily regenerated via calcination. In addition, this catalytic reduction system was found to minimize undesired repolymerization reactions (Van den Bosch et al. 2017).

2.7 Conclusion

This chapter provided an overview of the main hydrogenolysis-based technique – i.e., reductive catalytic fractionation (RCF) – used to convert native lignin into compounds with low molecular weight using Ni-based catalysts. The commercialization of lignin-derived fuels and chemicals necessitates the development of catalysts that increase the selectivity of C-O bond hydrogenolysis products while limiting monomer re-polymerization. However, the complex physiological properties of lignocellulosic biomass present a formidable challenge. Therefore, a catalyst system that is active, selective, and cost-effective is required.

To convert lignocellulosic biomass to fuels and chemicals, scientists and engineers have exerted a great deal of effort in this area of research and developed many cost-effective Ni catalysts due to the excellent hydrogenation/hydrolysis activities of nickel. However, catalyst efficiency and stability still show room for improvement. For lignin valorization, bifunctional catalysts with metal active sites and acid sites, such as Ni/Al_2O_3, have recently afforded promising results.

Given that the metal active sites and acid properties of the support can be tuned, thereby increasing the stability and selectivity toward platform monophenolics, the incorporation of earth-abundant promoters such as Cu and Fe -- which offer attractive synergetic effects when alloyed with Ni – represents a compelling way to advance lignin catalytic depolymerization research.

This study investigates the ability of Cu and Fe to enhance the performance of a 20% Ni/alumina catalyst in the reductive catalytic depolymerization of lignin present in whole cell biomass (i.e., native lignin) to phenolic monomers in sub- and super-critical methanol. Saliently, catalyst characterization – through techniques including N_2-physisorption, X-ray diffraction, and temperature-programmed reduction and desorption – were used in an effort to identify the structure-activity relationships underlying the performance of these catalysts in the reductive depolymerization of lignin.

CHAPTER 3. MATERIALS AND METHODS

3.1 Commercial chemicals and materials

All commercially available chemicals were used as received without additional purification. Dichloromethane (99.5%), tetrahydrofuran stabilized with BHT (99%), hexane (98.5%), methanol (99.8%), isopropyl alcohol (99%) and sulfuric acid (95-98%) were purchased from BDH VWR Chemicals. *N, O*-bis(trimethylsilyl)trifluoroacetamide (98.5%) and ethanol (100%) were purchased from Sigma Aldrich. Pyridine (99%) was purchased from Fisher Scientific. The analytical grade calibration standards purchased to quantify results obtained from liquid product analysis are listed in Table 3.1.

Nickel (II) nitrate hexahydrate and iron (III) nitrate nonahydrate were purchased from Alfa Aesar. Copper (II) nitrate trihydrate was purchased from Sigma Aldrich. SASOL provided γ-alumina (BET surface area of 210 m^2/g). De-ionized water (DI) was used in the reaction systems.

Debarked hybrid poplar (NM6) wood shavings were obtained from the University of Wisconsin.

Table 3.1. Analytical grade authentic standards purchased to quantify monomeric products in lignin oil via GC-MS.

Analytical standards	Purity (%)	Supplier
4-n-Ethyl guaiacol	98	Sigma Aldrich
4-n-Ethyl syringol	95	Sigma Aldrich
4-n-Propanol guaiacol	97	Sigma Aldrich
4-n-Propanol syringol	95	Sigma Aldrich
4-n-Propyl guaiacol	99	Sigma Aldrich
4-n-Propyl syringol	95	Sigma Aldrich
Coniferyl alcohol	98	Sigma Aldrich
Eugenol	99	Sigma Aldrich
Ferulic acid	99	Oakwood chemical
Guaiacol	99	Sigma Aldrich
Isoeugenol	98	Sigma Aldrich
Methyl 2-(4-hydroxy-3,5-dimethoxyphenyl) acetate	95	Chemspace
Methyl homovanillate	95	Sigma Aldrich
Syringaldehyde	98	Sigma Aldrich
Syringol	99	Sigma Aldrich
Syringyl alcohol	97	Fisher Scientific
Vanillic acid	97	Sigma Aldrich
Vanillin	99	Acros Organics

3.2 Pretreatment and compositional analysis of lignocellulose

Using a high-speed electric grain mill grinder (Amazon.com), milling and sieving procedures were performed to reduce and homogenize the size of air-dried lignocellulose such that it could pass through a 300-micron sieve.

Adapted from Van den Bosch et al. (2017), a Soxhlet extraction was executed to remove extractives, such as, fats, resins, waxes, and terpenoids/steroids that can affect subsequent determination of Klason lignin.

Typically, 2-3 g of finely sieved biomass was loaded into a fritted glass thimble and extracted in a KIMAX Soxhlet extraction apparatus with a mixture of toluene and ethanol (1:1). In a typical Soxhlet extraction, the extraction thimble containing the sample is gradually filled with condensed fresh solvent from the distillation flask because of the solvent reaching boiling temperature in the closed system (i.e., reflux). Once the thimble is submerged in the solvent, a siphon aspirates the contents of the thimble and carries it back into the distillation flask, which is then repeated until complete extraction is achieved (Luque de Castro and García Ayuso 2000). The initial introduction of solvent to the thimble via condensation takes a considerable amount of time, therefore, prior to a 24-hour extraction, a wet step was introduced in which samples were completely submersed in the solution to improve the overall speed of extraction. Once cooled to room temperature ($\leq$ 24 °C), the samples were washed with approximately 150 mL of hexane and then dried overnight in a vacuum oven at 80 °C.

The amount of lignin contained in lignocellulose was determined by the Klason lignin method. In lignin depolymerization literature, product yields are typically based on the amount of acid insoluble lignin, also known as Klason lignin, present in the lignocellulose sample (Abu-Omar et al. 2021). Adapted from Van den Bosch et al. (2017) and performed in triplicate, approximately 1 g of previously extracted biomass was transferred to a 25 mL flask after which 15 mL of 72 wt.% sulfuric acid solution was added along with a magnetic stir bar. The mixture was continuously stirred at room temperature for 2 hours.

With 60 mL of DI water, the contents of the flask were transferred to a 500 mL round bottom flask containing 300 mL of DI water – resulting in a 3 wt.% concentration of sulfuric acid solution. The diluted solution was boiled for 4 hours under reflux conditions, to maintain constant volume and acid concentration, and then left to cool to room temperature overnight. The brown lignin precipitate retained after vacuum filtration of the acid solution was then washed with hot DI water (approx. 85-99 °C) to remove any residual acid (determined with pH strips). The obtained solids were then dried in a vacuum oven at 80 °C overnight. The lignin content was determined relative to the oven dried substrate (i.e., acid insoluble lignin) by averaging the measured weight of the oven dried substrates (Equation B1).

The S/G content of lignin was determined at the National Renewable Energy Laboratory (NREL). Approximately 4 mg of extractive-free lignocellulose samples were pyrolyzed using a Frontier PY2020 unit at 500 °C for 30 seconds in 80 µL deactivated stainless steel cups and analyzed in duplicate. Mass spectral data was acquired using an Extrel Super-Sonic MBMS Model Max 1000 and processed using Merlin Automation software (V3). Spectra were collected from m/z 30 to 450 at 17 eV. Lignin content was estimated relative to a representative NIST standard of known Klason lignin content by summation of mean-normalized ion intensities of m/z 120, 124 (G), 137 (G), 138 (G), 150 (G), 152, 154 (S), 164 (G), 167 (S), 168 (S), 178 (G), 180, 181, 182 (S), 194 (S), 208 (S) and 210 (S) where G denotes primarily guaiacyl-derived ions, S denotes primarily syringyl-derived ions, and other ions either derive from other lignin monomers or multiple sources. Syringyl to guaiacyl (S/G) ratios were determined by dividing the sum of S-based ions by the sum of G-based ions using mean-normalized ion intensities (Harman-Ware et al. 2020).

The elemental contents of the lignocellulose were measured with a LECA CHN628 and a micro thermogravimetric analyzer (TA instruments, Inc.).

3.3 Catalyst preparation

Catalysts were prepared via excess wetness impregnation. The metal precursors for the catalysts were Ni $(NO_3)_2$ • $6H_2O$, Fe $(NO_3)_3$ • $9H_2O$, and Cu $(NO_3)_2$ • $3H_2O$, with γ-Al_2O_3 (BET surface area of 210 m^2 g^{-1}) serving as the support material. Nickel loading was held constant at 20 wt.% across all metal catalysts, and metal promoter loading was held constant at 5 wt.% across all catalysts. Contents were added to a round bottom flask and mixed with approximately 15 mL of DI water for 3 hours. The DI water was then removed via rotary evaporation and catalyst samples were dried further in a vacuum oven at 60 °C overnight. The green catalyst was then calcined at 500 °C for 3 hours in static air, and then finely ground to pass through a 150-micron sieve.

For simplicity, these catalysts will be henceforth referred to as Ni-only, Ni-Cu, and Ni-Fe, respectively.

3.4 Catalyst characterization

All catalyst characterization measurements were performed using calcined catalyst samples. The elemental compositions of catalyst samples were analyzed by Inductively Coupled Plasma Optical Emission Spectroscopy (ICP-OES) (Hou et al. 2021) on a Varian 720-ES analyzer equipped with a Sample Preparation System (SPS3) autosampler.

Prior to ICP-OES analysis, 0.1 g of catalyst sample was weighed into a Polytetrafluoroethylene (PTFE) beaker before adding 10 mL each of hydrochloric and nitric acids. The solution was digested on a hotplate (90 °C) for at least 30 minutes or until the liquid level had condensed to 5 mL. The samples were then cooled to room temperature and diluted to a total of 25 mL. Osmium was employed as the internal standard to improve the accuracy of the analytical data by correcting for variability between calibration standards and samples.

Textural properties such as surface area and pore volume of the catalysts were analyzed through N_2-physisorption (Bowker 1998) on a Micromeritics Tri-Star 3000 analyzer. A sample of 100 mg of catalyst was degassed at 160 °C under N_2 flow in a Micromeritics Flow Prep 060 degasser. The degassed sample was then subjected to N_2-physisorption at -196 °C. Results were calculated through the Brunauer-Emmett-Teller (BET) method to determine the surface area and pore volume (Brunauer, Emmett, and Teller 1938; Bowker 1998).

The average crystallite, or particle, size of the NiO nanoparticles was calculated by applying the Scherrer equation (Patterson 1939) to the NiO peaks observed in powder X-ray diffractograms, which were acquired using Phillips X'Pert diffractometer using Cu Kα radiation at λ=1.54 Å (0.154 nm) and a step size of 0.02°.

The following temperature programmed techniques were performed on a Micromeritics AutoChem II analyzer. The reducibility of the catalysts was studied using temperature-programmed reduction (H_2-TPR) analysis (Pirola, Galli, and Patience 2018).

A 100 mg sample of green catalyst was placed in a U-shaped quartz reactor and heated in a reducing atmosphere (100 cm/min of a mixture of 10% H_2 and 90% Ar) at a constant heating rate of 10 °C/min to a final temperature of 900 °C. The temperature was monitored using a thermocouple positioned in the catalyst bed. Changes in the hydrogen concentration at the reactor outlet were recorded using a thermal conductivity detector (TCD). After the catalysts were reduced at 350 °C (the same reduction temperature used in the catalytic depolymerization experiments), the amount of metallic Ni present on the surface of the catalyst samples was assessed using H_2 chemisorption. Adapted from Morgan et al. (2012), 250 mg of fresh catalyst was reduced under 10% H_2/Ar flow at 350 °C for 1 hour. The U-shaped quartz reactor was then purged with Ar at 450 °C for 30 minutes and then cooled under flowing Ar to 45 °C. Once the TCD signal stabilized, 0.025 mL (STP) of 10% H_2/Ar was then pulsed into the Ar carrier gas flowing to the reactor at 50 mL/min flowing through the catalyst. Pulsing was continued at 3-minute intervals until the area of the H_2 peaks remained constant. Temperature-programmed desorption of ammonia (NH_3-TPD) measurements were performed to assess the acid sites on the catalyst surface. A mass spectrometer detector (Thermostar) was employed to track several m/z signals, namely m/z = 44, 28, and 15, respectively corresponding to CO_2, CO, and NH_3 (CO_2 contributions to m/z 28 were subtracted to afford the NH_3-TPD trace). Prior to NH_3 adsorption, calcined catalysts were reduced at 350 °C for 3 hours under a flow of 10% H_2/Ar (60 mL/min), adsorbed hydrogen was removed from the surface by flushing the system at 450 °C for 30 minutes with 60 mL/min of Ar, and the catalyst bed was cooled to 50 °C using the same gas flow. At that temperature, NH_3 adsorption was conducted by flowing 50 mL/min of 1% NH_3/N_2 for 1 hour.

Following that, the system was purged for 1 hour with 100 mL/min of Ar to remove physically adsorbed NH_3. TPD measurements were then performed by raising the catalyst temperature from 50 to 500 °C at a rate of 10 °C/min. The area under the curve was integrated to determine the total acidity of the sample from its NH_3 desorption profile.

3.5 Catalytic activity testing

3.5.1 RCF experiments

Prior to depolymerization experiments, 100 mg of catalyst powder (particle size <150 μm) was added to a 50 mL stainless steel stirred batch microreactor (Parr Instruments Co.). After removing all traces of oxygen by flushing the reaction vessel three times with H_2, the vessel was sealed, and the catalyst was reduced at 350 °C for 3 hours in the presence of 10 bar of static hydrogen. Upon completion of the 3-hour reduction step, the reactor was cooled with an ice bath to room temperature. To prevent the re-oxidation of the now metallic Ni (e.g., Ni^0) catalyst back to NiO (e.g., Ni^{2+}), the following steps were taken to reduce the amount of oxygen drawn into the reactor upon addition of 25 mL of methanol and 1 g of lignocellulose (particle size <300 μm) for depolymerization experiments: (1) Three purges were performed with Ar to remove any lingering H_2 and provide an anaerobic barrier for the catalyst (Note: at STP, the density of Ar and O_2 is 1.78 g/L and 1.43 g/L, respectively): (2) Methanol and lignocellulose were added to the reactor in quick succession after the vessel was opened: and (3) The reactor was quickly resealed and purged three times with H_2 before being pressurized to 30 bar H_2 and heated to the desired reaction temperature of 200 or 250 °C.

The reaction temperature was measured by a type-J thermocouple housed in the reactor body. Mechanical stirring of 750 RPM was maintained by a magnetic stirrer during each experiment. At the end of these reactions (t_0; T = 200 or 250 °C), which lasted 3 hours, an ice bath was used to cool the reactor to room temperature (24 °C) before depressurizing the system. After the reaction, the monomers were extracted by DCM and analyzed by the procedures below.

3.5.2 Product separation and characterization

Separation of the solid fraction, containing carbohydrate pulp and the spent catalyst, from the liquid fraction, containing the lignin oil and some soluble sugar products was done via vacuum filtration (40-mesh filter paper). To collect the entire liquid fraction, the solid fraction was washed with additional methanol (approx. 40 mL). Methanol was removed from the filtrate via rotary evaporation to yield a brownish oil containing some soluble sugar products as well as phenolic monomers and oligomers, hereafter referred to as 'crude oil.'

The recovered solids are the fraction of the total biomass that were insoluble in methanol following the reaction. Polysaccharides make up most of these solids. Because the catalyst is difficult to separate from this solid combination, the weight of the catalyst was deducted from the total weight of dried solids (Equation B2). After separation, the solid product mixture was washed with methanol as stated above and dried in an oven overnight at 60 °C. The recovered solids composed of spent catalyst and carbohydrate pulp were submitted for CHN analysis to determine the elemental composition of the recovered solids.

The crude oil was dissolved in a solution of equal parts DI water and DCM at a volume ratio of 1/3/3 (crude oil/DCM/water) to separate the soluble sugars present in the water phase from the lignin-derived products present in the DCM phase. Approximately 5 mL of brine (a typical saturated solution of DI water and $NaCl_2$) was added to improve separation. After the DCM phase was separated, the water phase was extracted two additional times with approximately 10 mL of DCM each time. Each separated DCM phase was subjected to additional filtration and passed through anhydrous magnesium sulfate to remove any residual water. After separation, DCM was removed via rotary evaporation. The resulting oil yield, defined as lignin oil, which contained both phenolic monomers and oligomers, was used as a metric to describe the extent of lignin extraction (i.e., delignification degree).

3.5.3 GC-MS analysis of liquid products

The product distribution and quantification of detectable monomeric products was determined using a Gas Chromatograph (GC, Agilent 7890) coupled with a Mass Spectrometer detector (MS, Agilent 5975C). The column used in the GC was a 70 DB-1701 (60 m x 0.25 mm x 0.25 μm or 15 m x 0.25 mm x 0.25 μm as appropriate). The carrier gas was helium, and the flow rate was set to 1 mL/min for the 15 m column. The inlet temperature for the 60 m column was maintained at 300 °C using a method consisting of 45 °C for 3 min, a ramp to 280 °C at 4 °C/min, and a 10-minute hold. The inlet temperature of the 15 m column was kept at 280 °C with a temperature ramp of 60 °C to 80 °C at 2 °C/min, then to 110 °C at 3 °C/min, followed by a 20 °C/min ramp to 190 °C, and finally at 2 °C/min, reaching 230 °C.

The lignin oil was initially dissolved in tetrahydrofuran (THF) (5 mg/mL), and then dissolved further depending on the opacity of the scintillation vial to avoid clogging the GC column. Quantification of monomeric products in lignin oil samples was performed using Enhanced Chemstation Software (Agilent Technologies, Inc.). Commercially obtained analytical standards (Table 3.1) and n-dodecane were used to develop an internal standard calibration method. For non-commercially available monomers (such as sinapyl alcohol and 4-propenyl syringol), response factors were inferred based on the response factor on analogues. Product identification was conducted using the spectra library of the National Institute of Standards and Technology (NIST, Version 2014).

Analytical standard solutions were prepared with THF in which the concentration of each of the standard solutions were approximately 10 mg/mL. At least six calibration levels were performed by dilution of the stock solution for each standard compound ranging from 0.03 to 2 mg/mL. Prior to GC-MS analysis, all aliquots of lignin monomer standards, lignin oil products, and respective calibration samples were derivatized using 100 µL of BSTFA and subsequently heated in an oven at 60 °C for at least 30 minutes; a few drops of pyridine were used to catalyze the trimethylsilyation (TMS) reaction. The yield and selectivity of monomers were calculated using Equation B4 and Equation B5, respectively. The yield of oligomers was determined gravimetrically as the difference in mass between the lignin oil and phenolic monomers (Equation B6).

CHAPTER 4. RESULTS AND DISCUSSION

4.1 Catalyst characterization

The characterization of the three catalyst types were similar, regardless of the addition of Cu or Fe, shown in the textural properties and metal dispersion (Table 4.1) and in the metal loading (Table 4.2). It was observed that the additional Cu or Fe had minimal effect on the textural properties of the promoted Ni catalyst. Consistent with their total metal loadings and the fact that all catalysts were prepared using the same alumina support, the surface area, pore volume, and pore size of all catalysts fall in narrow ranges. Consequently, the effects caused by the minor differences in these properties on catalyst performance should also be minimal.

Table 4.1. Textural properties and metal dispersion of the fresh catalysts studied.

Active Phase	N_2 Physisorption			Avg. NiO particle size (nm)*
	BET surface area (m^2/g)	Pore volume (cm^3/g)	Avg. pore diameter (nm)	
Ni-only	170	0.30	5.8	4.2
Ni-Cu	165	0.28	5.7	9.6
Ni-Fe	185	0.32	5.8	3.9

*As measured from the powder X-ray diffractograms of the catalysts calcined under static air for 3 h at 500 °C.

Table 4.2. Elemental composition of the catalysts* studied via ICP-OES.

Active Phase	Metal Loading (%)	
	Nominal	Measured**
Ni-only	20	21.9
Ni (Cu)	20 (5)	21.9 (5.51)
Ni (Fe)	20 (5)	20.5 (4.35)

*Calcined under static air for 3 h at 500 °C; **Measurements taken in triplicate (SD: Ni-only = ± 1.3; Ni-Cu = ± 0.1, 0.6; Ni-Fe = ± 0.1, 0.6).

Figure 4.1 depicts the X-ray diffractograms of the fresh catalysts. The diffractograms were recorded with fresh catalysts in their oxidized (as opposed to reduced) form, therefore it is unsurprising that all Ni observed is in the form of NiO. Indeed, the three diffractograms exhibit many peaks at 37.2°, 43.3°, 62.9°, 75.4°, and 79.4°, which correspond to NiO (Vizcaíno, Carrero, and Calles 2007). Diffraction peaks corresponding to Fe_3O_4, and Ni-Fe alloy phases are absent from the diffractogram of the Ni-Fe catalyst because these phases are only expected in reduced catalysts (Yu, Chen, and Ren 2014; Han et al. 2019; Vizcaíno, Carrero, and Calles 2007; Wang et al. 2011). Additionally, the absence of peaks associated with Fe_2O_3 indicates that Fe is highly dispersed. Similarly, the absence of peaks associated with a CuO phase (Carrero, Calles, and Vizcaíno 2007) in the diffractogram of the Ni-Cu catalyst is also attributable to Cu being highly dispersed (Vizcaíno, Carrero, and Calles 2007; Lee et al. 2004).

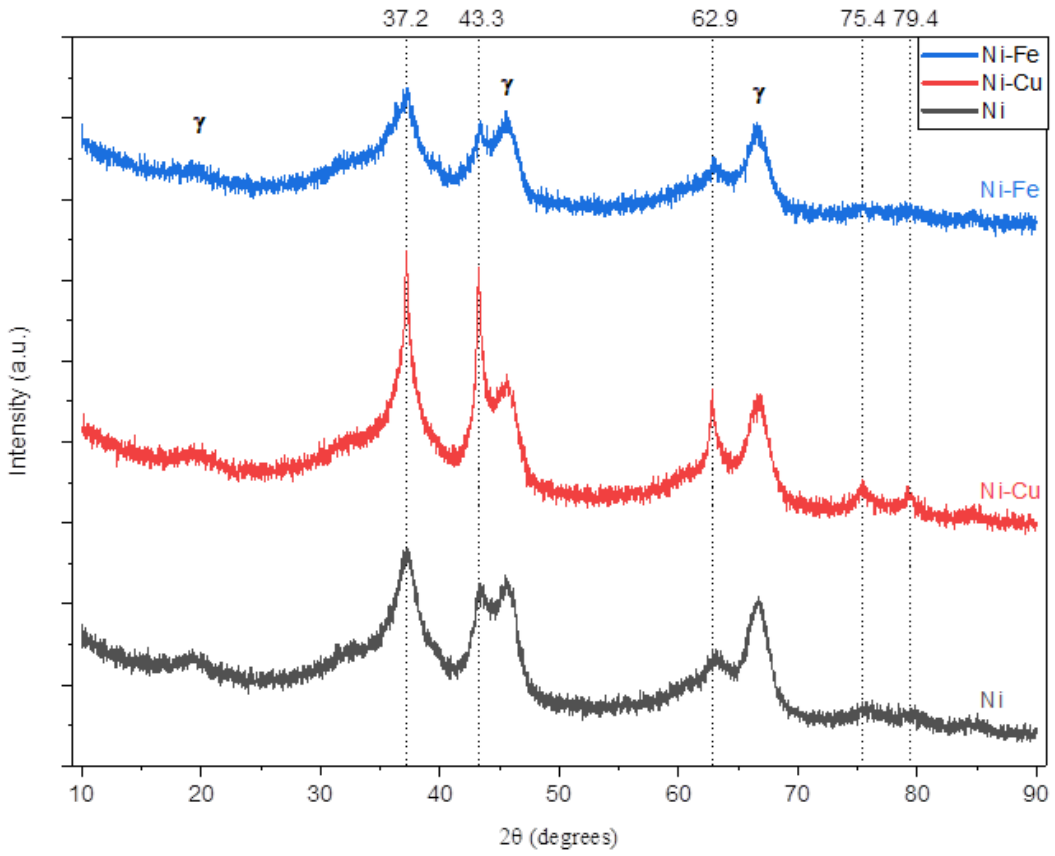

Figure 4.1. X-ray diffraction patterns of alumina supported catalysts. Ni-only (grey, bottom), Ni-Cu (red, middle), and Ni-Fe (blue, top). The dotted lines indicate NiO peaks and γ symbol indicates alumina support peaks.

The influence of promoter addition on the average particle size of NiO was investigated by applying the Scherrer equation to the NiO peak at 37.2° in each X-ray diffractogram shown in Figure 4.1. Notably, the NiO particle size in the Ni-Cu catalysts (9.64 nm) was much larger than the NiO particle size in the Ni-only and Ni-Fe formulations (4.21 and 3.86 nm, respectively). This is congruent with the findings of Loe et al. (2016), who reported that the Cu promotion led to an increase in the NiO particle size.

The TPR profiles depicted in Figure 4.2, indicate that both Cu and Fe promotion lowers the reduction temperature of NiO in the catalyst under study. The TPR profile for the monometallic Ni catalyst reveals three different reduction events: (1) a small signal with a local maximum at 240 °C attributable to the reduction of large Ni ensembles (Rynkowski, Paryjczak, and Lenik 1993); (2) a broad reduction peak attributable to the reduction of NiO to metallic Ni, with a maximum of 575 °C (Rynkowski, Paryjczak, and Lenik 1993); and (3) an indistinct shoulder around 700 °C attributable to the reduction of a nickel aluminate phase ($NiAl_2O_4$) which is formed from the reaction of NiO with the alumina support (Zieliński 1982). The TPR profile for the Ni-Cu catalyst reveals five main reduction events: (1) a sharp peak at 180 °C attributed to the reduction of copper oxide to copper metal (Vizcaíno, Carrero, and Calles 2007; Loe et al. 2016); (2) a definite shoulder with a local maximum at 225 °C indicating the reduction of large NiO and/or NiO-CuO ensembles (Rynkowski, Paryjczak, and Lenik 1993); (3) a broader peak with a maximum at 390°C attributed to the reduction of a NiO-CuO phase (Li et al. 1998); (4) another broad peak with a local maximum at 500 °C attributed to the reduction of NiO to Ni metal (Rynkowski, Paryjczak, and Lenik 1993); and (5) a small shoulder around 700 °C signaling the reduction of a $NiAl_2O_4$ phase (Zieliński 1982). In summary, the addition of Cu decreases the reduction temperature of NiO, consistent with previously reported observations (Loe et al. 2016). In turn, the decrease in the reduction temperature of Ni caused by the addition of Cu results in the formation of more Ni(0) or active metal sites on the surface of the catalyst (Loe et al. 2016).

The TPR profile for Ni-Fe also reveals several reduction events, including: (1) a small and broad peak at 225 °C corresponding to the reduction of large NiO ensembles; (2,3) an exceptionally large and broad peak ranging from 300 °C to 675 °C with a more prominent peak at 360 °C and a broader peak at around 550 °C, which represents the simultaneous reduction of iron oxide and nickel oxide leading to the formation of a Ni-Fe alloy (Yu, Chen, and Ren 2014); and (4) another small shoulder around 700 °C attributed to the reduction of a $NiAl_2O_4$ phase (Zieliński 1982).

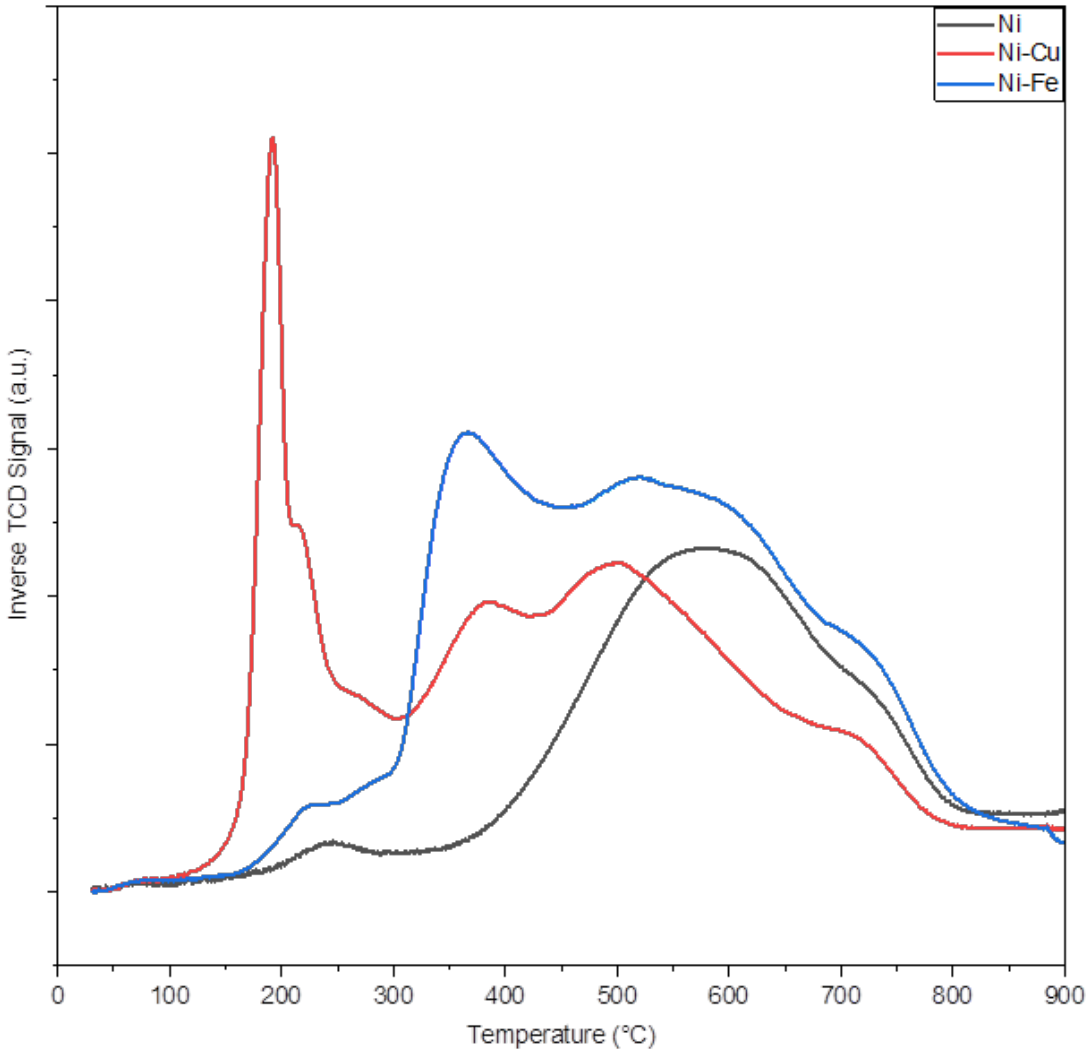

Figure 4.2. Temperature programmed reduction profiles of alumina supported Ni-only (grey), Ni-Cu (red), and Ni-Fe (blue) catalysts.

H_2 chemisorption was performed on the catalysts utilized in this investigation to determine the number of active sites on the catalyst surface after reduction at 350°C (the reduction temperature employed before catalyst testing). Table 4.3 displays the measured H_2 uptake for each catalyst, the Ni specific surface area calculated from uptake of H_2, and the amount of metal active sites (calculated based on the assumption of H_2 dissociative adsorption (Yang and Whitten 1993)).

Table 4.3 Pulsed H_2 chemisorption results of the catalysts screened for the depolymerization of lignin.

Active Phase	H_2 Adsorbed, (mL/g STP)	Ni specific surface area (m^2/g)	No. of active metal sites per g catalyst
Ni-only	0.09	3.05	$4.7x10^{18}$
Ni-Cu	0.20	6.98	$1.1x10^{19}$
Ni-Fe	0.12	4.26	$6.6x10^{18}$

The promotion of Ni with Fe merely boosts the uptake of H_2 from 0.09 to 0.12 mL/g and increases the number of adsorption sites from $4.7x10^{18}$ per gram to $6.6x10^{18}$ per gram. In contrast, the promotion of Ni with Cu raises the uptake of H_2 from 0.09 to 0.20 mL/g and augments the number of adsorption sites from $4.7x10^{18}$ per gram to $1.1x10^{19}$ per gram. The greater amount of H_2 adsorbed at this temperature achieved through the addition of Cu is consistent with the lower reduction temperature displayed by the Ni-Cu catalyst relative to its Ni-only and Ni-Fe counterparts.

The acidic properties of the catalyst samples were studied using the temperature-programmed desorption of ammonia (NH_3-TPD). The NH_3-TPD profiles acquired are shown in Figure 4.3. Relative to the reference Ni-only sample, the Ni-Cu and Ni-Fe NH_3-TPD profiles show a greatly reduced area under the curve,

which suggests that the addition of Cu or Fe considerably diminishes surface acidity (as confirmed by the values in Table 4.4). For these catalysts, the chemical make-up of the support material is the main source of catalyst acidity (Verhaak, van Dillen, and Geus 1993). Acid sites are expected to be neutralized due to the introduction of promoters (Bowker 1998) and thus, the reduced acidity of Ni-Cu and Ni-Fe catalysts was to be expected. In other words, since the acid sites are associated with the alumina support, the fact that acidity decreased upon addition of Cu or Fe to Ni suggests that these metals occupy acid sites that remain available in the monometallic Ni catalyst. Notably, this is not an undesirable result. Indeed, acidic supports typically favor char formation (Narani et al. 2015), which makes it important to moderate acidity.

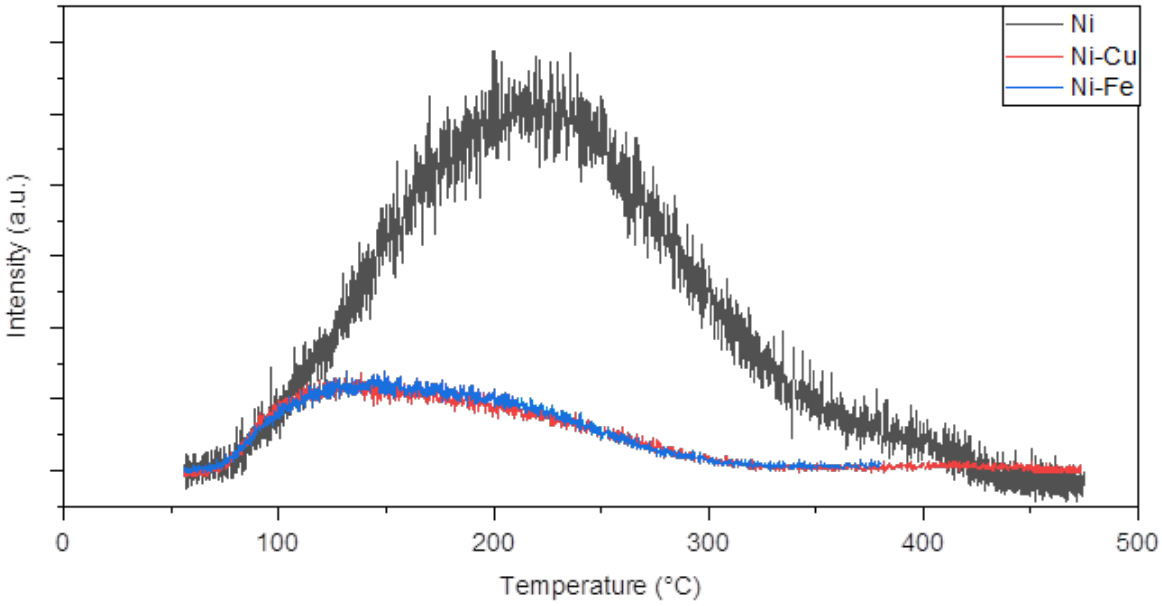

Figure 4.3. Temperature programmed desorption of ammonia profiles of alumina supported Ni-only (grey), Ni-Cu (red), and Ni-Fe (blue) catalysts.

Table 4.4. Relative acidity* of the fresh catalysts screened for lignin depolymerization.

Active phase	Acidity, μmol/g catalyst
Ni-only	205
Ni-Cu	47.7
Ni-Fe	53.3

*Estimated by applying Equation B8 to NH_3-TPD profiles in Figure 4.3.

4.2 Catalytic activity testing

In an effort to determine how the Cu or Fe promotion of alumina-supported Ni catalyst impacts their ability to depolymerize native lignin to monophenols, we investigated their performance in the reductive depolymerization of lignin contained in hybrid poplar lignocellulose at two temperatures (200 and 250 °C) corresponding to sub- and supercritical methanol (T-critical = 239 °C; P-critical = 81 bar).

These tests were carried out using a Ni/γ-alumina catalyst (with a metal loading of 20 wt.% for Ni and 5 wt.% for Cu and Fe) prepared in-house. Such supported Ni catalysts have displayed promising performance in hydrotreating experiments (Van den Bosch et al. 2017). Furthermore, the use of Ni as an active phase not only helps to stabilize lignin monomers, but also helps to generate hydrogen via the methanol reforming reaction ($CH_3OH+H_2O->CO_2+3H_2$). Promoted Ni catalysts are also advantageous due to their low cost in comparison to precious metals, to which Ni exhibits comparable yields when promoted with Fe or Cu (Chen et al. 2019).

Hybrid poplar (NM6) is a short-rotation woody crop characterized by its rapid growth and promising potential as an alternative source of renewable energy due to its high S-type monolignol content. Lignin that is primarily composed of S-type monolignols, such as hardwoods, contains a higher proportion of easily cleavable β-O-4 bonds, which are the primary linkage targeted for depolymerization (Schutyser et al. 2018). Therefore, genetically modifying poplar to contain an even greater abundance of S-type monolignols, as is the case with NM6 hybrid poplar, should result in higher yields of low molecular weight products. Therefore, NM6 hybrid poplar represents an excellent substrate to test the depolymerization efficiency of the catalysts in this study.

The critical conditions of methanol are lower than those of water, which offers a pathway to supercritical reactions performed under milder conditions. Supercritical methanol has not only been found to be an efficient medium for converting woody biomass to lower molecular weight products (Minami and Saka 2003; Minami, Kawamoto, and Saka 2003), but it can also work synergistically with Ni-Cu catalysts to facilitate the complex set of chemical reactions required for lignin depolymerization (Barta et al. 2010).

While monomer yield is a key indicator of the amount of usable lignin that can be converted into fuels and chemicals, the degree of lignin extraction can be quantified by calculating the total lignin oil yield (Equation B3). In addition, the yield of residual carbohydrate solids reveals the level of polysaccharide solubilization.

4.3 Influence of process conditions and catalyst promotion

4.3.1 Product yields

Figure 4.4 depicts the monomer yields and degree of saturation of the propene side chain of the aromatic monomers produced over the Ni-only, Ni-Cu, and Ni-Fe formulations, as well as in the absence of a catalyst (blank runs) at the two reaction temperatures investigated. The yield of lignin oil and recovered solids is also depicted.

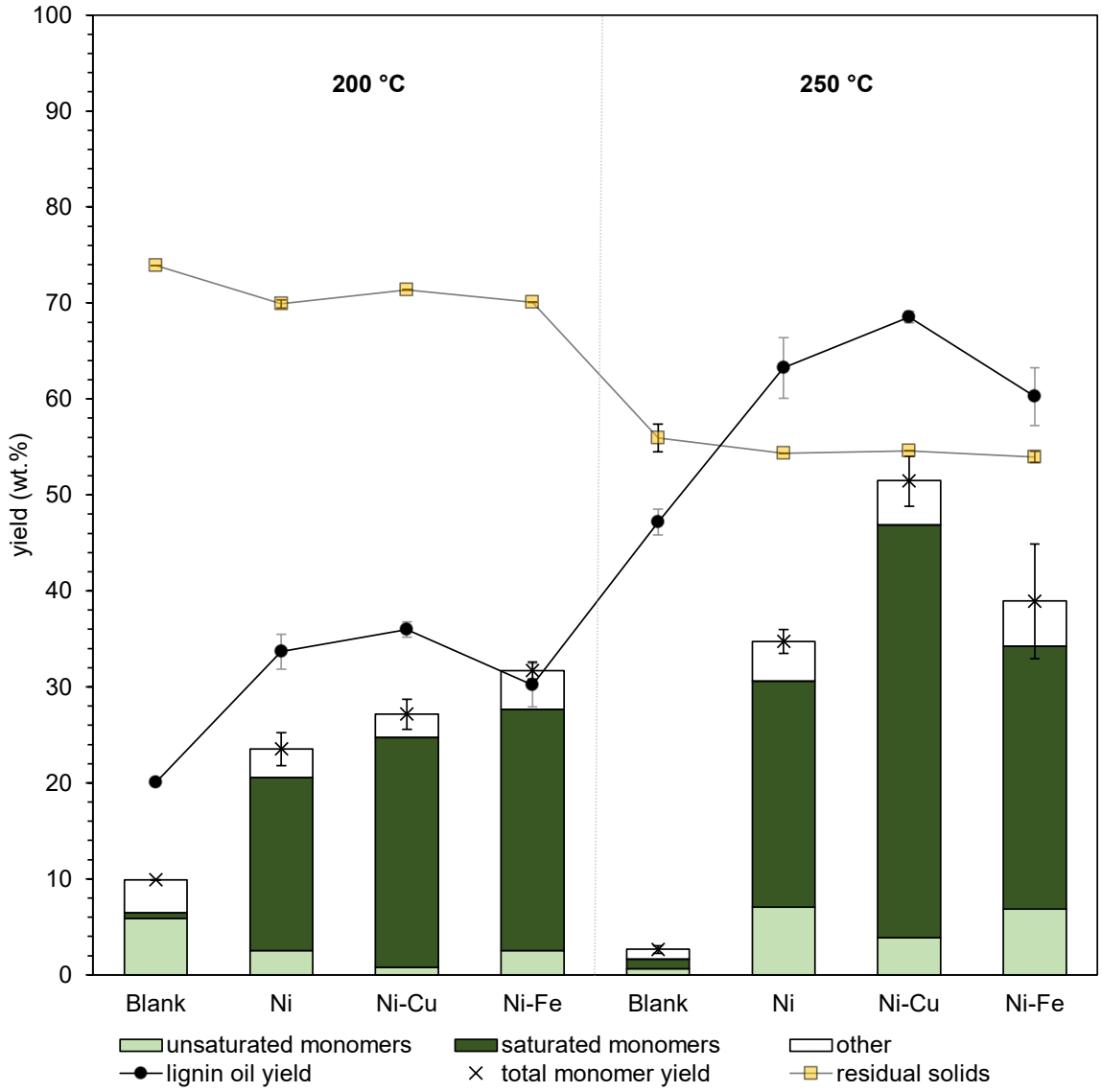

Figure 4.4. Poplar RCF over Ni-based catalysts. Total monomer yields ('x'), lignin oil yield (black circle), and solids retention (yellow square) are shown. The yield of saturated and unsaturated propyl aromatic monomers by weight is respectively shows in dark and light shading on the bars. The white fraction of the bars designated as 'other' corresponds to methyl paraben (MP)- and p-hydroxybenzoate (pHBA)-derived compounds, as well as to phenolic aldehydes/acids. All yields are from 3-h reactions in methanol at 200 or 250 °C.

The high selectivity to saturated monomers is consistent with the fact that Ni is an active hydrogenation catalyst at these conditions (Anderson et al. 2016). Promotion with Fe resulted in the maximum yield (32 wt.%) of monomers at 200 °C, but also in the lowest degree of delignification (30 wt.%) observed among the catalyzed runs performed at this temperature. Meanwhile, the Ni-Cu catalyst afforded the highest degree of delignification (36 wt.%), but a reduced yield of monomers relative to the Ni-Fe formulation (27 vs. 32 wt.%). The Ni-only catalyst performed comparably to Ni-Cu in terms of delignification (34 vs. 36 wt.%), but in terms of monomer yield it only produced 23.5 wt.%, which is the lowest among all catalysts tested at 200 °C. The presence of promoters does not seem to significantly impact the yield of recovered solids at 200 °C.

The depolymerization activity of the Ni catalysts was also investigated at 250 °C. At this temperature, methanol is in the supercritical phase. The autogenous pressure is 80 bar at the start of the reaction (when the temperature reaches 250 °C). Regarding the yield of lignin oil, similar patterns were observed at both 200 and 250 °C, indicating that the introduction of promoters has a similar effect on the degree of delignification irrespective of the reaction temperature. However, the lignin oil yield was higher overall at 250 °C than at 200 °C, which makes clear that lignin oil yield can be increased through the use of supercritical conditions. Supercritical methanol improves the solubility of lignocellulose, facilitating the formation of dissolved feedstock molecules as well as the reaction of the latter on the catalyst surface when a catalyst is present.

At 250 °C, the Ni-Cu catalyst afforded the maximum degree of delignification (68.5 wt.%) and a monomer yield of 51.4 wt.%, which is among the highest reported to date (Table 2.4). The minimal improvement of yields observed going from 200 to 250 °C over the Ni-only and Ni-Fe formulations relative to the much more pronounced yield increase obtained using the Ni-Cu catalyst could be attributed to the considerably higher number of active sites on the surface of the latter catalyst (Table 4.3), which appears to be effective at blocking secondary degradation reactions at higher temperature. In addition, the Ni-Cu catalyst displays higher selectivity to saturated products relative to the Ni-only and Ni-Fe formulations, which is indicative of an enhanced hydrogenation activity. The latter can stem from a synergetic effect between Cu and the supercritical methanol reaction medium resulting in improved hydrogen transfer on the surface of the catalyst, a similar phenomenon to that previously reported by other authors (Barta et al. 2010). It has also been reported that Ni-Cu alloys favor C-O bond cleavage over C-C bond breaking (Gandarias et al. 2012).

4.3.2 Mass balance

The mass balances of these experiments were >80% at 200 °C and >70% at 250 °C (Figure 4.5). Losses are primarily assigned to the gases evolved during reaction, which could not be accurately quantified and thus were not factored into the mass balance calculation (Equation B7). A precipitate encrusted on the reactor walls that was both hard to recover and quantify was produced for the reactions performed at 250 °C.

The formation of this precipitate is indicative of re-polymerization reactions that would be favored by higher temperatures, which could also lead to increased gas formation. The production of solids and gases difficult to recover and quantify explains the lower mass balances observed at 250 °C.

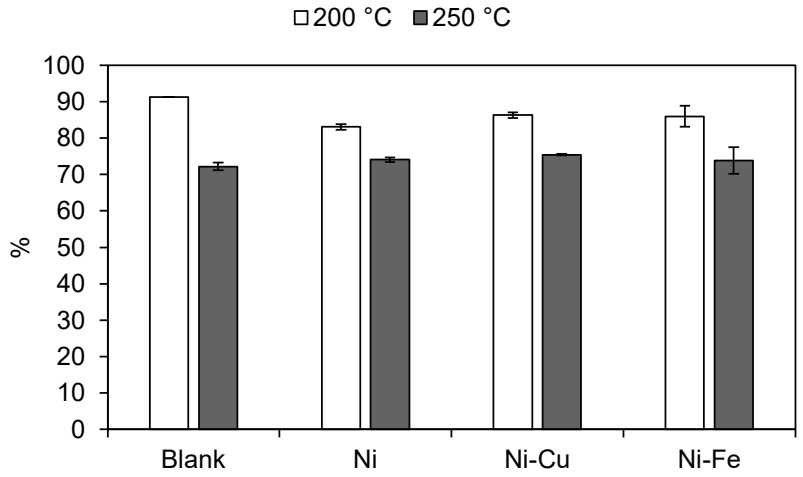

Figure 4.5. The influence of process conditions and catalyst promotion on the mass balance for products produced from poplar RCF. White and grey bars represent mass balances calculated at 200 and 250 °C, respectively.

4.3.3 Blank runs

Poplar was subjected to the reaction conditions described in this chapter in the absence of a catalyst to determine the extent to which the depolymerization of lignin proceeds solvothermally as opposed to catalytically. Indeed, the results from these blank (sans catalyst) runs can be used to identify the contributions of catalytic and non-catalytic (solvothermal) effects to the yield of different monomers (Figure 4.6). When temperature is increased from 200 to 250 °C, the total monomer yield declines drastically (10 wt.% to 3 wt.%), which is contrary to the trend observed in the presence of Ni-based catalysts (Figure 4.4).

The significantly lower monomer yields obtained in these blank runs in general – and in the blank supercritical run in particular – highlights the advantages of using a Ni-based catalyst. Although monomer yields in blank runs are low and decline with increasing temperature, lignin oil yields are higher and follow a similar temperature pattern to that displayed by catalyzed runs. Recovered solids are also highest for blank runs, which is most likely due to lignin being extracted from lignocellulose but not depolymerized into low molecular weight aromatics. This is consistent with the conclusions of Sun et al. (2018), who compared the gel permeation chromatography data from uncatalyzed and catalyzed processes.

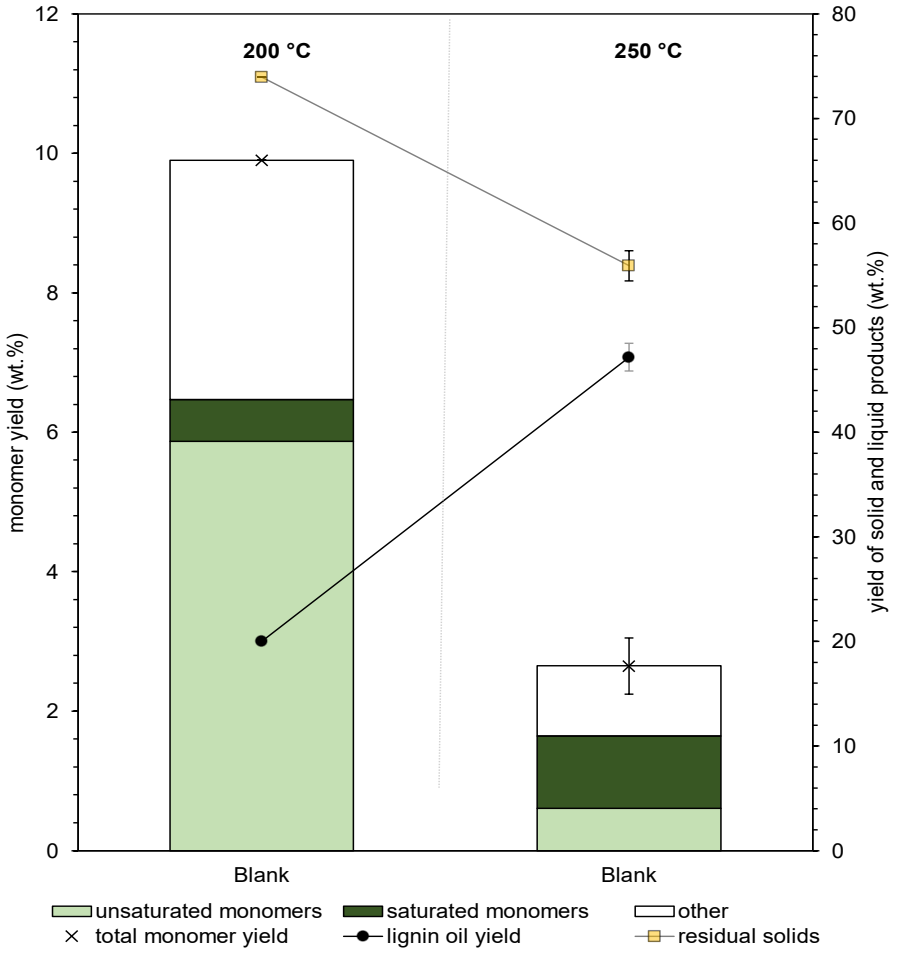

Figure 4.6. Solvothermic (sans catalyst) reactions with poplar. Total monomer yields ('x'), lignin oil yield (black circle), and solids retention (yellow square) are shown. The yield of saturated and unsaturated propyl aromatic monomers by weight is respectively shows in dark and light shading on the bars. The white fraction of the bars designated as 'other' corresponds to methyl paraben (MP)- and p-hydroxybenzoate (pHBA)-derived compounds, as well as to phenolic aldehydes. All yields are from 3-h reactions in methanol at 200 or 250 °C.

4.3.4 Distribution of monomers

The primary products obtained in the solvothermal (sans catalyst) reactions at 200 °C are coniferyl and sinapyl alcohols, which have been identified recently as key intermediates in the reductive conversion of native lignin (Anderson et al. 2017; Van den Bosch et al. 2017; Kumaniaev et al. 2017; Renders et al. 2018). Other monomeric products include guaiacol and syringol (G/S), ethyl-G/S, propyl-G/S, propenyl-G/S, and propanol-G/S (Figure 4.7). These unsaturated compounds are formed solvolytically (as opposed to catalytically) but have been reported to be unstable reaction intermediates at elevated temperatures (Van den Bosch et al. 2017), which is consistent with the fact that no coniferyl or sinapyl alcohols were obtained at 250 °C (Figure 4.8).

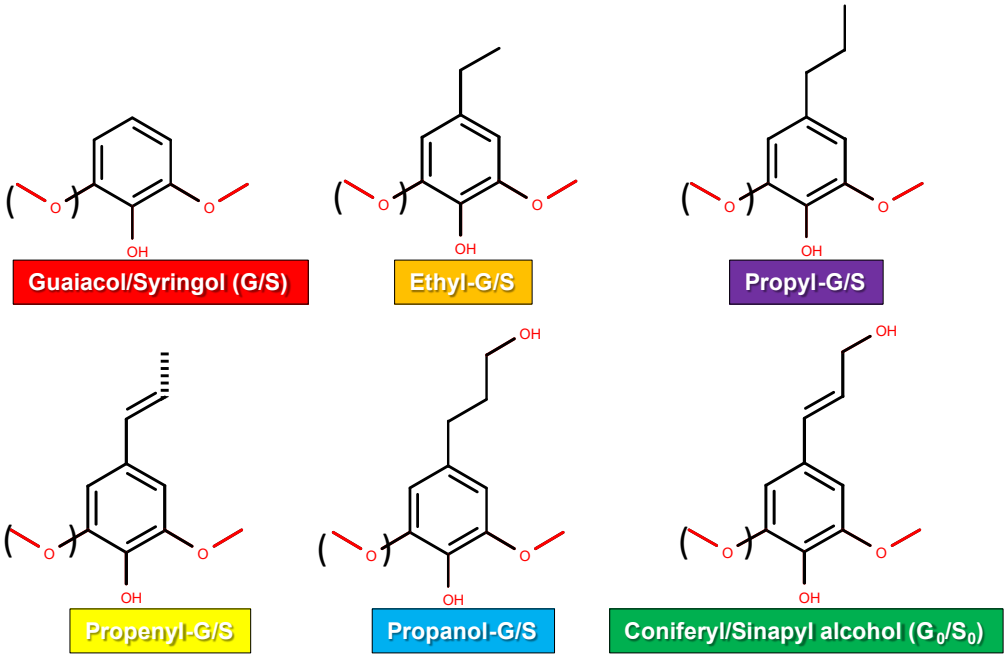

Figure 4.7. The primary monomers obtained from RCF of poplar. Colors and abbreviations are used henceforth. Note: Guaiacol has one methoxy group and syringol has two methoxy groups which is distinguished by the presence of the parentheses.

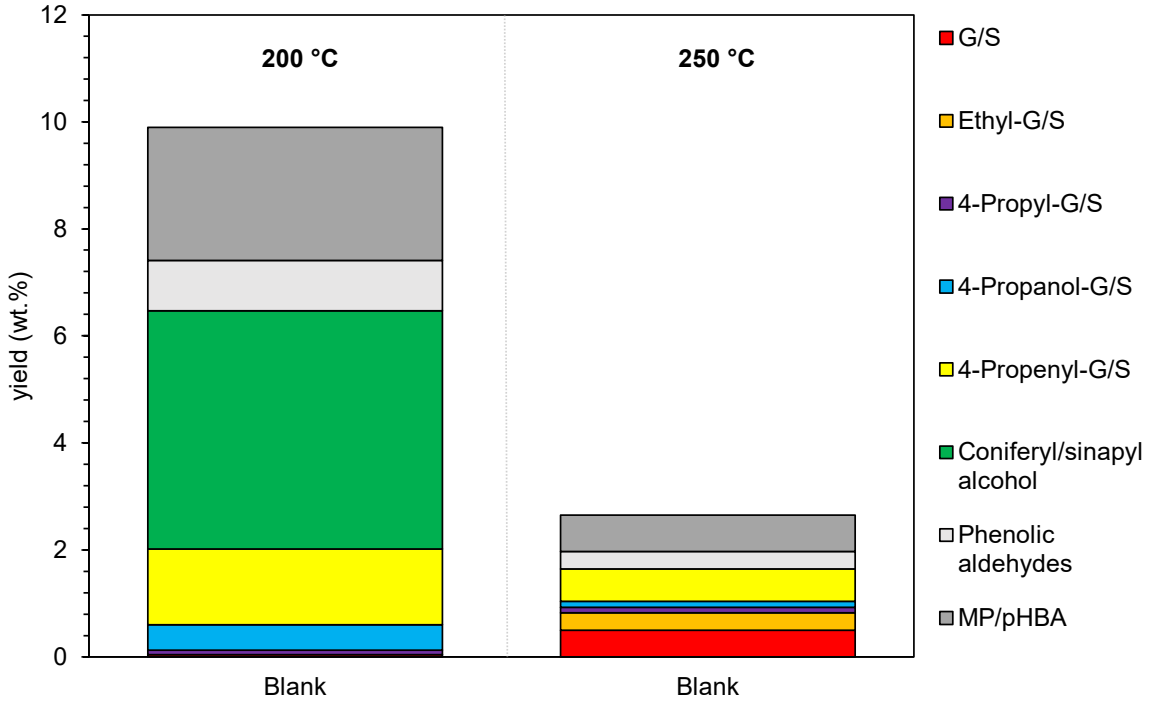

Figure 4.8. Comparison of the monomer yields obtained at various temperatures in the absence of catalysts.

Renders et al. (2018) proposed a reaction network for native lignin conversion in which the formation of coniferyl/sinapyl alcohol serves as a crucial step in the depolymerization process. These authors concluded that the formation of propyl-G/S occurs primarily through the hydrogenolysis of coniferyl/sinapyl alcohol followed by the hydrogenation of the C_α=C_β double bond as indicated in their proposed reaction network, which is depicted in Scheme 1. The reaction network includes the following pathways: native lignin is first solvolytically depolymerized in the absence of a redox catalyst forming coniferyl/sinapyl alcohol (R1), which then either undergoes hydrogenation of the double bond to form propanol-G/S (R2), or undergoes hydrogenolysis of the terminal hydroxy group to form propenyl-G/S.

Renders et al. (2018) found that reaction conditions consisting of exogenous hydrogen, a carbon-supported ruthenium redox catalyst, and 200 °C did not induce the conversion of the propanol side chains to propyl (R5). Instead, these authors found that the formation of propyl sidechains more likely occurs through the hydrogenolysis of coniferyl/sinapyl alcohol followed by hydrogenation of the propenyl double bond (R3+R6). Against this backdrop, Figure 4.9 depicts the distribution of monomeric products obtained in the presence of Ni catalysts. More detailed information of the monomers obtained is tabulated in Appendix C.

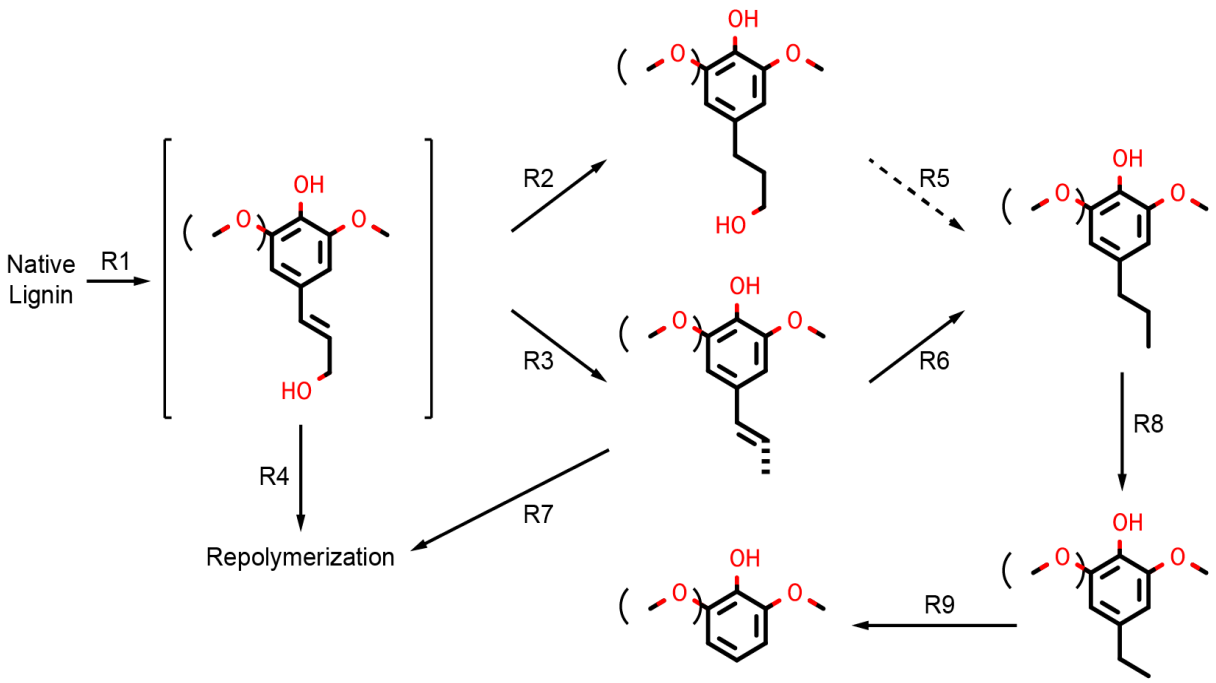

Scheme 1. Reaction network for the conversion of native lignin adapted from (Renders et al. 2018).

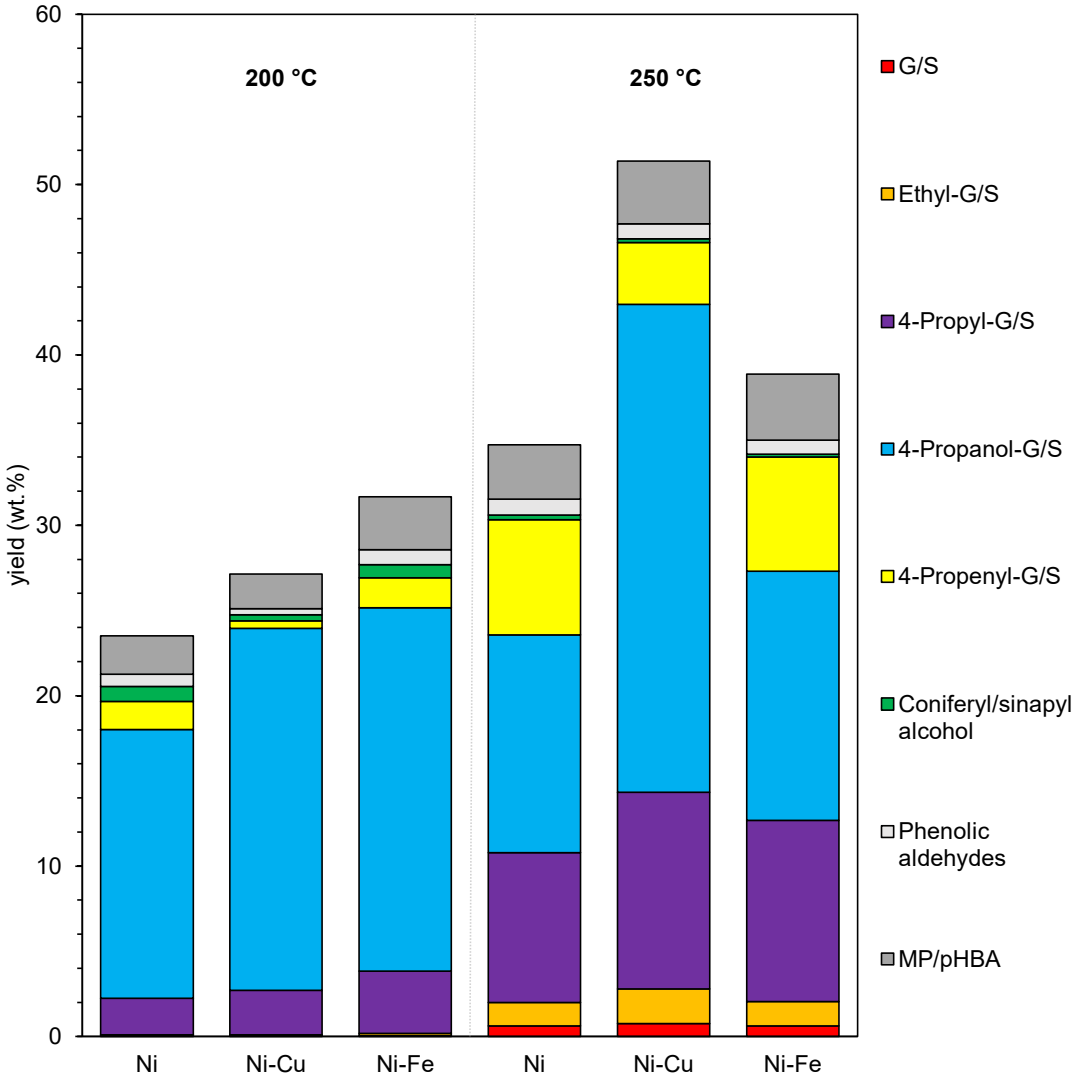

Figure 4.9. Comparison of the monomer yields of reactions performed at various temperatures using supported Ni-based catalysts.

Monomeric products obtained at 200 and 250 °C primarily consist of propanol-, propenyl-, and propyl-substituted monomers derived from guaiacol and syringol (denoted as 'G/S' in Figure 4.9). This is in line with previous reports in which these have been reported as the predominant products obtained in the presence of a redox catalyst and similar reductive conditions (Groß et al. 2021; Schutyser et al. 2018; Schutyser et al. 2017).

In addition, other authors have reported that Ni catalysts supported on alumina promote the production of propanol sidechains (Van den Bosch et al. 2017). When the temperature is increased from 200 to 250 °C, the selectivity for propyl-substituted sidechains increases, which has also been reported in the literature (Renders et al. 2018). The high yield of aromatic monomers suggests that aromatic ring was not hydrogenated and the high selectivity to phenols is also indicative of moderate hydrogen consumption, both of these being optimal outcomes of reductive reactions (Zakzeski et al. 2010). The Ni catalysts investigated in this study are therefore effective in the reductive catalytic depolymerization of native lignin.

The increased monomer yields observed at 250 °C are attributable to several factors related to the use of hydrogen as the reaction atmosphere and of methanol as the reaction solvent. Hydrogen stabilizes reactive free radicals produced by the thermal depolymerization of lignin and saturates the side chain functionalities of phenols leading to a reduction in repolymerization, which in turn inhibits the formation of coke on the catalyst surface and minimizes coke-induced deactivation (Bai and Kim 2016). In addition, methanol acts as a H-donor, the high level of H-donor species present in the reaction medium as a result of increased partial pressure at 250 °C increasing the yield of monomers and selectivity to side chain reduction products such as propanol-G/S (Shen et al. 2016). The higher selectivity to propyl-sidechains at 250 °C may be attributed to the fact that methanol is known to inhibit catalytic hydrogenation without affecting the hydrogenolysis of ether bonds, thereby enhancing the selectivity of monophenols derived from lignin (Shen et al. 2016).

Aside from the overall increase in monomer yields observed at 250 °C, the primary difference observed between reactions performed at 200 and 250 °C pertains to the formation of ethyl-G/S and guaiacol/syringol (G/S) in the presence of Ni-based catalysts at 250 °C. This may be due to an increase in the cracking activity of Ni resulting in the dealkylation of the propane side chain. Tellingly, the blank (sans catalyst) run performed at 250 °C produced ethyl-G/S and G/S at similar selectivity to the catalyzed runs (Table 4.5). This means that the more stringent reaction conditions can also increase cracking activity on their own, although Ni is known to be an active cracking catalyst in hydroprocessing reactions. There is also a higher selectivity to propyl-G/S at 250 °C. This may result from a higher partial pressure of hydrogen generated by increasing temperature and thus methanol reforming. Indeed, Barta et al. (2010) found that methanol reforming increased in the presence of Cu and supercritical methanol. Ouyang et al. (2019) found that the gas phase primarily contained hydrogen, CO, and CO_2, and confirmed that hydrogen yield increased with temperature due to increased methanol reforming, providing a good explanation for the increased rate of double bond hydrogenation in the presence of Ni-Cu at both temperatures as evidenced by the higher selectivity to saturated monomers. Consistent with the results of Kenny et al. (2022), p-Hydroxybenzoic acid methyl ester (pHBA) and methyl paraben (MP) (likely synthesized via decarboxylation of pHBA) were produced during the RCF reactions. Similar levels of pHBA and methyl paraben were detected for all 3-hour reactions regardless of H_2 pressure, indicating that routes from pHBA are independent of external hydrogen at high conversions, regardless of process conditions or catalyst promotion.

Table 4.5. Influence of process conditions and catalyst promotion on selectivity to monomers.

Temp (°C)	Sample	S/G ratio*	Selectivity (%)					
			G_0/S_0	Propanol	Propenyl	Propyl	Ethyl	G/S
-	Raw poplar	1.6						
200	Blank	3.2	45	4.8	14	0.9	0	0.4
	Ni	1.5	3.7	67	7.0	9.2	0.3	0.1
	Ni-Cu	1.5	1.3	78	1.6	9.7	0.2	0.1
	Ni-Fe	1.5	2.4	67	5.6	12	0.4	0.1
250	Blank	4.8	0	4.1	23	4.1	12	19
	Ni	2.0	0.8	37	19.5	25	4.0	1.8
	Ni-cu	1.8	0.4	56	7.1	22	4.0	1.5
	Ni-Fe	1.8	0.5	38	17	27	3.7	1.6

* S/G ratio was calculated as the sum of S-derived monomers divided by the sum of G-derived monomers. S/G ratio of raw poplar was measured via thiacidolysis to serve as a reference.

At 200 and 250 °C the main products are syringol-derived monomers (Appendix C), which was to be expected. The lignin fraction of poplar lignocellulose, which is a hardwood, contains mainly syringyl (S) units and a relatively small amount of guaiacyl (G) units. The S/G ratio (1.6) of poplar was measured via thiacidolysis for benchmarking purposes. In the presence of Ni catalysts, the S/G ratios calculated from the monomeric products detected in the lignin oil resulted in ratios close to 1.6 (Table 4.5). Notably, the results of blank (sans catalyst) reactions demonstrate that the nickel catalysts were able to successfully depolymerize lignin to its constituent monophenols. Thus, results obtained clearly show that the Ni-based catalysts investigated are effective lignin depolymerization catalysts.

4.3.5 Recovered solids

Maximizing the utilization of the lignin and carbohydrate components of lignocellulosic biomass is a primary goal of technologies designed to valorize this feedstock. Consequently, a key step of the RCF of lignin is to determine the chemical composition of the extracted lignin oil as well as of the recovered solids. Figure 4.10 depicts the yields of recovered solids obtained in the experiments performed in this study, which represent the proportion of the total biomass that was insoluble in methanol following RCF. Yields are >70 wt.% and >50 wt.% at 200 and 250 °C, respectively. Catalyst promotion with Fe or Cu does not have a significant impact on the yield of recovered solids irrespective of the reaction temperature. The ash content of the recovered solids (detailed in Table 4.6) indicated that the latter stems mainly from the catalyst powder, but the fact that the value remains below 10% is notable because values above 10% are known to impact hydrolysis (Abu-Omar et al. 2021).

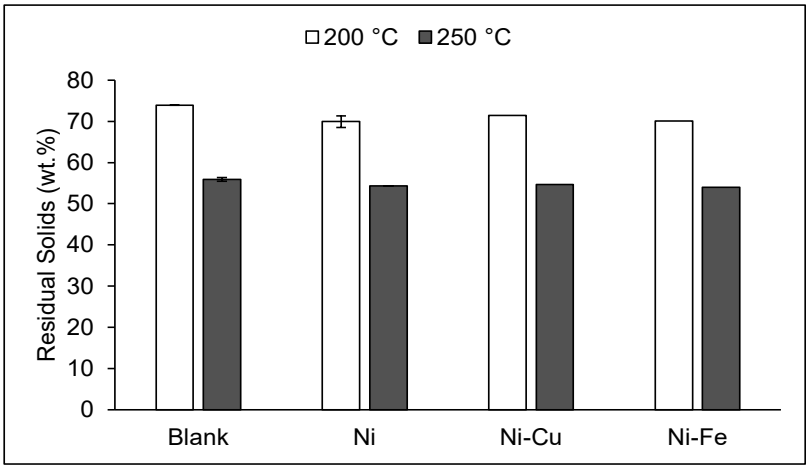

Figure 4.10. The influence of process conditions and catalyst promotion on the yield of recovered solids from RCF of poplar.

The low ash content of the recovered solids, which include the spent catalyst and cellulose pulp, is consistent with the efficient release of lignin from the cell wall while quenching reactive intermediates (Table 4.6). Quenching reactive intermediates is the primary role of an RCF catalyst. Accordingly, the Ni-based formulations studied being excellent catalysts for reductive lignin depolymerization is indicated by the low ash content present in the recovered solids. These solids are reported to be predominantly composed of polysaccharides (Anderson et al. 2016; Renders et al. 2018; Renders et al. 2016; Schutyser et al. 2015; Van den Bosch et al. 2017; Van den Bosch, Schutyser, Vanholme, et al. 2015; Parsell et al. 2015); however, enzymatic saccharification would be required to evaluate their suitability for fermentation to ethanol. Anderson et al. (2016) reported similar yields for recovered solid at 200 and 250 °C in the presence of a Ni catalyst. Moreover, these authors also found that supercritical methanol had a greater impact on sugar degradation concluding that milder process conditions (200 °C) may be best for biorefinery operations focused on maximizing the yield of both oil and solids.

There is a noticeable tradeoff between RCF occurring at 200 or 250 °C, i.e., although 250 °C (and supercritical methanol) result in increased monomer yields, recovered solids are significantly reduced. This highlights the link between biomass structure and the severity of process conditions. Notably, this study's overarching objective was to investigate the catalytic activity of Ni catalysts under optimal process conditions to improve the economics of the cellulosic ethanol biorefinery. Since the complete utilization of biomass carbohydrates and lignin is a prerequisite for deploying the RCF process in a biorefinery scheme (Bartling et al. 2021; Cooreman et al. 2020; Davis et al. 2018; Schutyser et al. 2017), the more moderate conditions at 200 °C, which produced a greater yield of recovered solids suitable for further processing to ethanol may be preferable.

Table 4.6. Results of elemental analysis on raw poplar lignocellulose and recovered solids from the RCF of poplar.

Temp (°C)	Sample	Elemental Composition (dry wt.%)						Proximate Analysis (dry wt.%)	
		C	H	N	O	S	Ash	Volatile Matter	Fixed Carbon
-	Raw poplar*	45.9	6.7	0.5	45.7	0.0	1.1	80.5	9.9
200	Blank	43.6	6.5	0.3	49.6	0.0	0.1	92.7	2.5
	Ni	40.0	5.8	0.2	47.8	0.0	6.3	82.4	6.3
	Ni-Cu	40.0	5.9	0.2	45.6	0.1	8.2	81.9	5.3
	Ni-Fe	39.2	5.6	0.2	45.1	0.1	7.5	82.4	5.1
250	Blank	46.4	6.1	0.2	45.9	0.0	1.3	85.8	8.3
	Ni	39.5	5.6	0.2	47.9	0.0	6.8	84.7	4.3
	Ni-Cu	39.3	5.7	0.2	46.2	0.0	8.5	83.5	4.3
	Ni-Fe	38.4	5.6	0.2	47.8	0.0	8.0	84.3	3.3

* Raw poplar sample taken as a reference to distinguish solvothermal effects.

CHAPTER 5. CONCLUSIONS AND RECOMMENDATIONS

5.1 Conclusions

The utilization of γ-Al_2O_3-supported Ni catalysts promoted with either Cu or Fe for the reductive catalytic fractionation (RCF) of hybrid poplar in methanol at 200 and 250 °C was investigated with the goal of improving biorefinery efficiencies. Monomer yields improved from 34.7% over 20% Ni/Al_2O_3 to 51.4% over 20% Ni-5% Cu/Al_2O_3 at 250 °C, indicating that Cu is a highly effective promoter of Ni-based catalysts for the reductive depolymerization of hybrid poplar in supercritical methanol. Metal particle size changes do not appear to be the cause of the improvements in RCF performance achieved with the addition of Cu to Ni catalysts. Instead, the improved performance obtained through Cu promotion can be attributed to the ability of Cu to facilitate the reduction of Ni leading to an increase in the amount of Ni^0 – which is thought to be the catalytically active phase for lignin depolymerization – on the catalyst surface.

Although Cu promotion and supercritical conditions can provide remarkable monomer yields, the latter is not the only consideration of importance to the overall economic viability of lignocellulosic biorefineries. Indeed, at least in the current iteration of lignocellulosic biorefineries, the primary target is the production of bio-ethanol from carbohydrates extracted from lignocellulose, where the lignin fraction is typically considered a lower value co-product. Thus, in view of the relatively low number of solids – a proxy for carbohydrates – recovered from experiments performed at 250 °C, it could be argued that lignin depolymerization at this temperature is less effective than that caried out under milder conditions.

Notably, while Fe or Cu promotion also improves monomer yields in experiments performed at 200 °C, only a slight impact on the amount of solids retained is observed at this temperature. Bartling et al. (2021) have recently concluded that polysaccharide retention in the carbohydrate rich pulps does not substantially affect the RCF oil minimum selling price (MSP) and noted that the high-pressure reactor required to operate in more stringent conditions contributes greatly to the total installed capital cost of a facility. In short, the best set of conditions will surely be dependent on the interplay between the value of different product streams and the cost of installing and operating the facility.

Saliently, this study showed that an approach that affords a clean carbohydrate residue can also efficiently catalyze the conversion of lignin present in the whole biomass to yield a number of phenolic compounds near the theoretical maximum. This was accomplished through a Ni-based system that cleaves and deoxygenates the β-O-4 bonds in native lignin under moderate reaction conditions. The dominant products found were propanol guaiacol, propanol syringol, propyl syringol, and propenyl-substituted guaiacol and syringol. Monophenols isolated from lignin can be converted into a variety of aromatic chemicals and fuels. Using this innovative lignin utilization approach would allow for biorefineries to produce more of these products. The development of a lignin-first biorefinery scheme for the production of fuels and chemicals indicates a shift in the biofuels production framework, where lignin may be more valuable than cellulose.

5.2 Recommendations and Future Work

Catalyst recovery, regeneration, and re-use, as well as reactor design for a variety of biomass feedstocks, could be areas of focus for future work on reductive catalytic fractionation over Ni-based catalysts. The catalysts spent in RCF can be successfully regenerated by removing the coke deposits accumulated on the catalyst surface leading to deactivation (Van den Bosch et al. 2017). The regeneration of the catalyst via calcination poses a challenge since metal particle sintering and/or metal redistribution may occur. Performing thermogravimetric analysis (TGA) on the spent catalysts would reveal information about the promoters' ability to prevent surface coking and thus coke-induced catalyst deactivation. Increased resistance to the latter may reflect the promoters' ability to reduce the cracking activity of Ni-only catalysts while also imparting superior selectivity to saturated monomers via geometric and electronic effects. Furthermore, assessing the loss of active sites due to the RCF reaction would be useful. Van den Bosch et al. (2017) observed that fouling of these active sites during RCF caused catalyst deactivation, but a reductive treatment of the spent catalyst restored the availability of the Ni sites. The characterization of the spent catalysts using N_2 physisorption and chemisorption studies would reveal the extent to which the textural properties (surface area and/or porosity) of the catalysts are altered during RCF. In short, regeneration/recyclability experiments of RCF catalysts would be an important aspect of process feasibility studies since they would demonstrate the benefit of using non-carbonaceous catalyst support materials to facilitate catalyst regeneration through the removal of coke species via calcination.

A dedicated study focused on support materials would also be informative. Liao et al. tested various commercial metal catalysts to hydroprocess propyl guaiacol (a surrogate for lignin oil) to phenol and observed that while acidic supports favored undesirable side products, silica was more selective than alumina at the same conversion levels (Liao et al. 2020). This suggests that investigating the effect of the catalyst support for Ni-Cu and Ni-Fe formulations to be used in the RCF of lignin would be of value.

To study catalyst regeneration and re-use, it is also important to consider the ease with which the catalyst can be recovered from the system after RCF, which is certainly a factor impacting the overall economics of the biorefinery. One approach that would facilitate catalyst recovery is the containment of catalyst pellets inside a basket system. Indeed, Van den Bosch et al. (2017) demonstrated that intimate contact between solid biomass and solid catalyst is not essential in RCF, concluding that catalysis is only required to avoid repolymerization reactions by hydrogenating unsaturated lignin intermediates to more stable phenolics. Thus, pellets of promoted Ni catalyst – which are both porous and mechanically stable – placed in a basket system could afford several advantages with respect to process design and scale-up such as facile catalyst recovery and clean pulp production suitable for downstream processing.

Process-wise, additional improvements could involve a flow-through semi-continuous reactor design similar to that reported by other authors (Anderson et al. 2017; Anderson et al. 2019; Stone et al. 2022). Saliently, a flow-based method facilitates the collection of both kinetic and mechanistic data, which is necessary to inform the design, development, and scaleup of the RCF process. Multi-bed RCF investigations can provide unique insights into the best way to avoid catalyst deactivation due to leaching, sintering, and surface poisoning, which result in increased concentrations of unsaturated lignin intermediates and an increase in the occurrence of oligomerization. Regardless of reactor design, future research should also include leaching studies on the lignin oil samples using ICP-OES or ICP-MS to ensure dissolved metals stemming from the catalyst or the reactor are not present in the final product. The utilization of a Hastelloy reactor would obviate one potential source of metals in solutions, i.e., those that may leach from the reactor wall during reaction (Abu-Omar et al. 2021).

Understanding the significance of the structural diversity of lignocellulosic biomass is also essential. The amount and type of biomass that can be used to produce materials and energy in a multipurpose biorefinery is determined by geographic location, crop rotation, as well as by limitations put in place by the energy density of crops on transportation. Since it is important to maximize the amount and type of biomass that can be employed, it is crucial to test the ability of Ni catalysts to depolymerize other forms of biomass, such as softwood and herbaceous species. Given that an agricultural waste residue such as corn stover contains additional extractives that may play a role in catalyst deactivation, additional data would need to be gathered regarding the durability of the catalyst.

By evaluating the RCF of this and other biomass feedstock over Ni-Cu and Ni-Fe catalysts, valuable information pertaining to catalyst activity, selectivity, stability, recyclability – and versatility – can be obtained.

The goal of a lignocellulosic biorefinery is to maximize the utilization of the major biomass constituents. As a result, efficient valorization via RCF is only justified if the carbohydrate pulp can be effectively utilized. To demonstrate the feasibility of using RCF pulp to produce bioethanol, efficient saccharification and fermentation of both cellulose and hemicellulose should be demonstrated. This can be accomplished by conducting digestibility tests with commercial cellulase cocktails. Future tecno-economic analysis (TEA) research should be informed by an analysis of the structural composition of the spent sample to quantify the carbohydrate fraction of the raw lignocellulose substrate free of extractives to determine the yield of polysaccharides preserved during RCF (Abu-Omar et al. 2021).

APPENDICES

APPENDIX A: List of abbreviations

Abbreviation	Definition
α	alpha
AC	activated carbon
AEO	Annual Energy Outlook
Al_2O_3	alumina oxide
$AlCl_3$	aluminum chloride
Ar	argon
Auto	autogenous pressure
β	beta
BET	Brunauer-Emmett-Teller
BHT	butylated hydroxytoluene
BSTFA	n,o-bis(trimethylsilyl) trifluoroacetamide
C	carbon
C-C	carbon-carbon bond
C-lignin	lignin composed primarily of caffeyl alcohol
CO	carbon monoxide
C-O	carbon-oxygen bond (ether bond)

Abbreviation	Definition
CO_2	carbon dioxide
Cu	copper
CuO	copper oxide
DCM	dichloromethane
DI water	de-ionized water
EISA	Energy Independence and Security Act (2007)
EohS	4-n-ethanol syringol
EPA	U.S. Environmental Protection Agency
ES	4-n-ethyl syringol
EtOH	ethanol
Fe	iron
Fe_2O_3	iron (III) oxide
Fe_3O_4	iron (II,III) oxide
γ	gamma
G	guaiacol
G_0	coniferyl alcohol
GC	gas chromatograph
G-unit	guaiacyl alcohol

Abbreviation	Definition
H_2	hydrogen
H_2O	water
H_3PO_4	phosphoric acid
HDO	hydrodeoxygenation
H-donor	hydrogen donor
HMF	hydroxymethylfurfural
H-unit	p-coumaryl alcohol
ICP	inductively coupled plasma
LA	levulinic acid
m/z	mass to charge ratio
MeOH	methanol
Mo	molybdenum
MP/pHBA	methyl paraben/ p-hydroxybenzoic acid methyl ester
MS	mass spectrometry
MSP	minimum selling price
Mt	million tons
N_2	nitrogen
$NaCl_2$	sodium chloride; salt

Abbreviation	Definition
NaOH	sodium hydroxide
NH_3	ammonia
Ni	nickel
Ni^0	metallic nickel
Ni_2P	nickel phosphide
$NiAl_2O_4$	nickel aluminate
NiO or Ni^{2+}	nickel oxide
NIST	National Institute of Standards and Technology
NM6	Populus maximowiczii x nigra
NMR	nuclear magnetic resonance
NP	not provided
NREL	National Renewable Energy Laboratory
O_2	oxygen
OES	optical emission spectroscopy
Pd	palladium
PohG	4-n-propanol guaiacol
PohS	4-n-propanol syringol
2-PrOH	2-propanol/ isopropanol

Abbreviation	Definition
PG	4-n-propyl guaiacol
PS	4-n-propyl syringol
PTFE	polytetrafluoroethylene
RCF	Reductive Catalytic Fractionation
Rh	ruthenium
R-Ni	Raney Nickel
RPM	revolutions per minute
Ru	rhodium
S	syringol
S/G ratio	relative amount of S and G in lignin
S_0	sinapyl alcohol
sc-solvent	supercritical-solvent
SiO_2	silicon dioxide
SPS3	sample preparation system
STP	standard temperature and pressure
S-unit	syringyl alcohol
TCD	thermal conductivity detector
TEA	techno-economic analysis

Abbreviation	Definition
TGA	thermogravimetric analysis
THF	tetrahydrofuran
TMS	trimethylsilyation
TPD	temperature-programmed desorption
TPR	temperature-programmed reduction
U.S.	United States
W	tungsten
WGS	water gas shift
X / Y	X = catalyst material; / = 'supported on'; Y = support material
XRD	x-ray diffractogram

APPENDIX B: List of equations

Equation B1. Klason lignin content

$$\text{Klason lignin (\%)} = \left(\frac{\text{wt. of acid insoluble lignin}}{\text{wt. of lignocellulose sample}}\right) \times 100\%$$

Equation B2. Yield of recovered solids

$$\text{Residual solids (\%)} = \left(\frac{\text{recovered solids wt. - catalyst wt.}}{\text{wt. of lignocellulose sample}}\right) \times 100\%$$

Equation B3. Degree of delignification

$$\text{Lignin oil yield (\%)} = \left(\frac{\text{wt. of lignin oil}}{\text{wt. of lignocellulose sample x Klason lignin}}\right) \times 100\%$$

Equation B4. Lignin monomer yield

$$\text{Monomer yield (\%)} = \left(\frac{\text{wt. of monomers}}{\text{wt. of lignocellulose sample x Klason lignin}}\right) \times 100\%$$

Equation B5. Product selectivity

$$\text{Selectivity to X monomer (\%)} = \left(\frac{\text{wt. of X monomer}}{\text{total sum of monomers}}\right) \times 100\%$$

Equation B6. Lignin oligomer yield

$$\text{Oligomer yield (\%)} = (\text{Lignin oil yield} - \text{Monomer yield})$$

Equation B7. Mass balance calculation

$$\text{Mass balance (\%)} = \left(\frac{(\text{recovered solids wt. - catalyst wt.}) + \text{crude oil wt.}}{\text{wt. of lignocellulose sample}}\right) \times 100\%$$

Equation B8. Relative acidity of the catalyst

$$\text{acidity } (NH_3\ \mu\text{mol/g}) = \left(\frac{\text{area of acid site}}{\text{RF } NH_3 \text{ calibration}}\right) \div g_{\text{catalyst}}$$

where RF is Response Factor

APPENDIX C: Detailed tabulation of product yields and distribution

Table C1. Effect of the reaction temperature on the distribution of monomers relative to total lignin content.

Catalyst type	Blank		Ni		Ni-Cu		Ni-Fe	
Monomer identification	Yield (wt.%) Temperature (°C)		Yield (wt.%) Temperature (°C)		Yield (wt.%) Temperature (°C)		Yield (wt.%) Temperature (°C)	
	200	250	200	250	200	250	200	250
Guaiacol (G)	0.0	0.0	0.0	0.0	0.0	0.0	0.0	0.0
4-Ethyl-G	0.0	0.0	0.0	0.1	0.0	0.1	0.0	0.1
4-Propyl-G	0.0	0.0	0.1	0.9	0.1	1.6	0.4	1.4
4-Propenyl-G	0.5	0.2	0.9	3.4	0.3	2.7	1.3	4.2
G4*	0.0	0.0	0.0	0.0	0.0	0.1	0.0	0.0
4-Propanol-G	0.1	0.1	7.0	5.7	9.3	12.4	9.1	6.4
Coniferyl alcohol (G_0)	0.9	0.0	0.3	0.1	0.2	0.1	0.3	0.1
Syringol (S)	0.0	0.5	0.0	0.6	0.0	0.8	0.0	0.6
4-Ethyl-S	0.0	0.3	0.1	1.3	0.1	1.9	0.1	1.4
4-Propyl-S	0.1	0.1	2.1	7.9	2.5	10.0	3.3	9.2
4-Propenyl-S	0.9	0.4	0.7	3.3	0.1	1.0	0.4	2.5
S4*	0.0	0.0	0.0	0.0	0.0	0.0	0.0	0.0
4-Propanol-S	0.3	0.0	8.7	7.1	12.0	16.2	12.2	8.2
Sinapyl alcohol (S_0)	3.5	0.0	0.6	0.2	0.2	0.1	0.4	0.1
Aldehydes*	0.9	0.3	0.7	0.9	0.4	0.9	0.9	0.8
MP/pHB	2.5	0.7	2.3	3.2	2.0	3.7	3.1	3.9
Total monomer yield	9.9	2.6	23.5	34.7	27.1	51.4	31.7	38.9
Oligomer yield	10.1	44.5	10.1	28.5	8.8	17.1	< 0	21.3
Lignin oil yield	20.0	47.2	33.7	63.2	36.0	68.5	30.2	60.3

Reaction conditions: 1 g of poplar, 0.1 g of catalyst, 25 mL methanol, 3 hr.
* G4 = methyl homovanillate; S4 = (3,5-Dimethoxy-4-hydroxyphenyl) acetic acid; aldehydes = vanillin, coniferyl aldehyde, sinapaldehyde, syringaldehyde

Table C2. Effect of the reaction temperature on the distribution of monomers relative to total lignin content.

Catalyst type	Blank		Ni		Ni-Cu		Ni-Fe	
Monomer identification	Yield (wt.%) Temperature (°C)		Yield (wt.%) Temperature (°C)		Yield (wt.%) Temperature (°C)		Yield (wt.%) Temperature (°C)	
	200	250	200	250	200	250	200	250
G/S	0.04	0.50	0.02	0.61	0.02	0.75	0.04	0.61
G_0/S_0	4.46	0.00	0.88	0.29	0.36	0.21	0.75	0.18
Ethyl-(G/S)	0.00	0.32	0.06	1.40	0.06	2.04	0.13	1.43
Propyl-(G/S)	0.09	0.11	2.16	8.77	2.64	11.55	3.66	10.63
Propenyl-(G/S)	1.41	0.61	1.65	6.77	0.43	3.65	1.78	6.69
Propanol-G/S	0.47	0.11	15.77	12.78	21.23	28.62	21.32	14.64
Other	3.43	1.00	2.98	4.12	2.40	4.62	4.01	4.73
Total monomer yield	9.90	2.65	23.52	34.73	27.15	51.44	31.69	38.91
Lignin oil yield	20.03	47.17	33.67	63.23	35.98	68.53	30.19	60.25
Solid pulp yield	73.93	55.92	69.91	54.33	71.38	54.61	70.09	53.97

Reaction conditions: 1 g of poplar, 0.1 g of catalyst, 25 mL methanol, 3 hr.

REFERENCES

Abo, Bodjui Olivier, Ming Gao, Yonglin Wang, Chuanfu Wu, Hongzhi Ma, and Qunhui Wang. 2019. 'Lignocellulosic biomass for bioethanol: an overview on pretreatment, hydrolysis and fermentation processes', *Reviews on Environmental Health*, 34: 57-68.

Abu-Omar, Mahdi M., Katalin Barta, Gregg T. Beckham, Jeremy S. Luterbacher, John Ralph, Roberto Rinaldi, Yuriy Román-Leshkov, Joseph S. M. Samec, Bert F. Sels, and Feng Wang. 2021. 'Guidelines for performing lignin-first biorefining', *Energy & Environmental Science*, 14: 262-92.

Alonso, David Martin, Stephanie G. Wettstein, and James A. Dumesic. 2012. 'Bimetallic catalysts for upgrading of biomass to fuels and chemicals', *Chemical Society Reviews*, 41: 8075.

Anderson, Eric M., Rui Katahira, Michelle Reed, Michael G. Resch, Eric M. Karp, Gregg T. Beckham, and Yuriy Roman-Leshkov. 2016. 'Reductive Catalytic Fractionation of Corn Stover Lignin', *Acs Sustainable Chemistry & Engineering*, 4: 6940-50.

Anderson, Eric M., Michael L. Stone, Max J. Hülsey, Gregg T. Beckham, and Yuriy Román-Leshkov. 2018. 'Kinetic Studies of Lignin Solvolysis and Reduction by Reductive Catalytic Fractionation Decoupled in Flow-Through Reactors', *ACS Sustainable Chemistry & Engineering*, 6: 7951-59.

Anderson, Eric M., Michael L. Stone, Rui Katahira, Michelle Reed, Gregg T. Beckham, and Yuriy Román-Leshkov. 2017. 'Flowthrough Reductive Catalytic Fractionation of Biomass', *Joule*, 1: 613-22.

Anderson, Eric M., Michael L. Stone, Rui Katahira, Michelle Reed, Wellington Muchero, Kelsey J. Ramirez, Gregg T. Beckham, and Yuriy Roman-Leshkov. 2019. 'Differences in S/G ratio in natural poplar variants do not predict catalytic depolymerization monomer yields', *Nature Communications*, 10.

Bai, Xianglan, and Kwang Ho Kim. 2016. 'Biofuels and Chemicals from Lignin Based on Pyrolysis.' in Zhen Fang and Jr Richard L. Smith (eds.), *Production of Biofuels and Chemicals from Lignin* (Springer Singapore: Singapore).

Barta, Katalin, Theodore D. Matson, Makayla L. Fettig, Susannah L. Scott, Alexei V. Iretskii, and Peter C. Ford. 2010. 'Catalytic disassembly of an organosolv lignin via hydrogen transfer from supercritical methanol', *Green Chemistry*, 12: 1640.

Bartling, Andrew W., Michael L. Stone, Rebecca J. Hanes, Arpit Bhatt, Yimin Zhang, Mary J. Biddy, Ryan Davis, Jacob S. Kruger, Nicholas E. Thornburg, Jeremy S. Luterbacher, Roberto Rinaldi, Joseph S. M. Samec, Bert F. Sels, Yuriy Román-Leshkov, and Gregg T. Beckham. 2021. 'Techno-economic analysis and life cycle assessment of a biorefinery utilizing reductive catalytic fractionation', *Energy & Environmental Science*, 14: 4147-68.

Bowker, M. 1998. *The Basis and Applications of Heterogeneous Catalysis* (Oxford University Press: Oxford).

Brunauer, Stephen, P. H. Emmett, and Edward Teller. 1938. 'Adsorption of Gases in Multimolecular Layers', *Journal of the American Chemical Society*, 60: 309-19.

Bulkowska, K., Gusiatin, Z.M., Klimiuk, E., Pawlowski, A., & Pokoj, T. (Eds.). . 2016. *Biomass for Biofuels (1st ed.)* (CRC Press).

Cao, Zhengwen, Michael Dierks, Matthew Thomas Clough, Ilton Barros Daltro De Castro, and Roberto Rinaldi. 2018. 'A Convergent Approach for a Deep Converting Lignin-First Biorefinery Rendering High-Energy-Density Drop-in Fuels', *Joule*, 2: 1118-33.

Carrero, A., J. A. Calles, and A. J. Vizcaíno. 2007. 'Hydrogen production by ethanol steam reforming over Cu-Ni/SBA-15 supported catalysts prepared by direct synthesis and impregnation', *Applied Catalysis A: General*, 327: 82-94.

Chen, Xiao, Weixiang Guan, Chi-Wing Tsang, Haoquan Hu, and Changhai Liang. 2019. 'Lignin Valorizations with Ni Catalysts for Renewable Chemicals and Fuels Productions', *Catalysts*, 9: 488.

Cooreman, E., T. Vangeel, K. Van Aelst, J. Van Aelst, J. Lauwaert, J. W. Thybaut, S. Van den Bosch, and B. F. Sels. 2020. 'Perspective on Overcoming Scale-Up Hurdles for the Reductive Catalytic Fractionation of Lignocellulose Biomass', *Industrial & Engineering Chemistry Research*, 59: 17035-45.

Crocker, Mark; Andrews, Rodney. 2010. 'The Rationale for Biofuels.' in M. Crocker (ed.), *Thermochemical Conversion of Biomass to Liquid Fuels and Chemicals* (RSCPublishing).

Davis, Kirsten, Marjorie Rover, Robert Brown, Xianglan Bai, Zhiyou Wen, and Laura Jarboe. 2016. 'Recovery and Utilization of Lignin Monomers as Part of the Biorefinery Approach', *Energies*, 9: 808.

Davis, Ryan E., Nicholas J. Grundl, Ling Tao, Mary J. Biddy, Eric C. Tan, Gregg T. Beckham, David Humbird, David N. Thompson, and Mohammad S. Roni. 2018. "Process Design and Economics for the Conversion of Lignocellulosic Biomass to Hydrocarbon Fuels and Coproducts: 2018 Biochemical Design Case Update; Biochemical Deconstruction and Conversion of Biomass to Fuels and Products via Integrated Biorefinery Path." In.: Office of Scientific and Technical Information (OSTI).

Dou, Xiaomeng, Wenzhi Li, Chaofeng Zhu, and Xiao Jiang. 2021. 'Catalytic waste Kraft lignin hydrodeoxygenation to liquid fuels over a hollow Ni-Fe catalyst', *Applied Catalysis B: Environmental*, 287: 119975.

Els, Frik. 2020. 'MINING.COM', Accessed October. https://www.mining.com/markets.

Fernando, Sandun, Sushil Adhikari, Chauda Chandrapal, and Naveen Murali. 2006. 'Biorefineries: Current Status, Challenges, and Future Direction', *Energy & Fuels*, 20: 1727-37.

Ferrini, Paola, and Roberto Rinaldi. 2014. 'Catalytic Biorefining of Plant Biomass to Non-Pyrolytic Lignin Bio-Oil and Carbohydrates through Hydrogen Transfer Reactions', *Angewandte Chemie International Edition*, 53: 8634-39.

Gale, Mark, Charles M. Cai, and Kandis Leslie Gilliard-Abdul-Aziz. 2020. 'Heterogeneous Catalyst Design Principles for the Conversion of Lignin into High-Value Commodity Fuels and Chemicals', *Chemsuschem*, 13: 1947-66.

Gandarias, I., J. Requies, P. L. Arias, U. Armbruster, and A. Martin. 2012. 'Liquid-phase glycerol hydrogenolysis by formic acid over Ni–Cu/Al2O3 catalysts', *Journal of Catalysis*, 290: 79-89.

Goacher, Robyn E., Yaseen Mottiar, and Shawn D. Mansfield. 2021. 'ToF-SIMS imaging reveals that p-hydroxybenzoate groups specifically decorate the lignin of fibres in the xylem of poplar and willow', *Holzforschung*, 75: 452-62.

Graça, Inês, Robert T. Woodward, Marco Kennema, and Roberto Rinaldi. 2018. 'Formation and Fate of Carboxylic Acids in the Lignin-First Biorefining of Lignocellulose via H-Transfer Catalyzed by Raney Ni', *Acs Sustainable Chemistry & Engineering*, 6: 13408-19.

Groß, Jonathan, Caroline Grundke, Johannes Rocker, Anthony J. Arduengo, and Till Opatz. 2021. 'Xylochemicals and where to find them', *Chemical Communications*, 57: 9979-94.

Han, Qiao, Mooeez Ur Rehman, Junhu Wang, Alexandre Rykov, Oliver Y. Gutiérrez, Yujun Zhao, Shengping Wang, Xinbin Ma, and Johannes A. Lercher. 2019. 'The synergistic effect between Ni sites and Ni-Fe alloy sites on hydrodeoxygenation of lignin-derived phenols', *Applied Catalysis B: Environmental*, 253: 348-58.

Hanson, Steve; Hill, Sean. 2018. "EPA finalizes Renewable Fuel Standard for 2019, relfecting cellulosic biofuel shortfalls." In *Today in Energy*. Washington, D.C.: U.S. Energy Information Administration.

Harman-Ware, Anne Elizabeth, Madhavi Martin, Nancy L. Engle, Crissa Doeppke, and Timothy J. Tschaplinski. 2020. "Rapid screening of secondary aromatic metabolites in Populus trichocarpa leaves." In.: Research Square Platform LLC.

Hingsamer, Maria, and Gerfried Jungmeier. 2019. 'Chapter Five - Biorefineries.' in Carmen Lago, Natalia Caldés and Yolanda Lechón (eds.), *The Role of Bioenergy in the Bioeconomy* (Academic Press).

Hou, Xiandeng, Renata S. Amais, Bradley T. Jones, and George L. Donati. 2021. 'Inductively Coupled Plasma Optical Emission Spectrometry.' in R.A. Meyers (ed.), *Encyclopedia of Analytical Chemistry* (John Wiley & Sons Ltd).

Huber, George W., Sara Iborra, and Avelino Corma. 2006. 'Synthesis of Transportation Fuels from Biomass: Chemistry, Catalysts, and Engineering', *Chemical Reviews*, 106: 4044-98.

Jacobs, Meg. 2016. *Panic at the Pump: The Energy Crisis and the Transformation of American Politics in the 1970s* (Hill and Wang: New York).

Jenkins, A., and N. K. Erraguntla. 2014. 'Vanillin.' in Philip Wexler (ed.), *Encyclopedia of Toxicology (Third Edition)* (Academic Press: Oxford).

Johnson, J.E. Holladay; J.J. Bozel; J.F. White; D. 2007. "Top Value-Added Chemicals from Biomass." In.: Pacific Northwest National Laboratory.

Jongerius, A.L. 2013. 'Catalytic Conversion of Lignin for the Production of Aromatics', Utrecht University.

Kannapu, Hari P. Reddy, Charles A. Mullen, Yaseen Elkasabi, and Akwasi A. Boateng. 2015. 'Catalytic transfer hydrogenation for stabilization of bio-oil oxygenates:reduction of p-cresol and furfural over bimetallic ni-cu catalysts using isopropanol', *Fuel processing technology*, 2015 v.137: pp. 220-28.

Kautto, Jesse, Matthew J. Realff, Arthur J. Ragauskas, and Tuomo Kässi. 2014. 'Economic Analysis of an Organosolv Process for Bioethanol Production', *BioResources; Vol 9, No 4 (2014)*.

Kenny, Jacob K., David Brandner, Sasha R. Neefe, William E. Michener, Yuriy Roman-Leshkov, Gregg T. Beckham, and Will Medlin. 2022. 'Catalyst choice impacts aromatic monomer yields and selectivity in hydrogen-free reductive catalytic fractionation', *Reaction Chemistry & Engineering*.

Kim, Jae-Young, Jeesu Park, Ung-Jin Kim, and Joon Weon Choi. 2015. 'Conversion of Lignin to Phenol-Rich Oil Fraction under Supercritical Alcohols in the Presence of Metal Catalysts', *Energy & Fuels*, 29: 5154-63.

Klein, Ian, Basudeb Saha, and Mahdi M. Abu-Omar. 2015. 'Lignin depolymerization over Ni/C catalyst in methanol, a continuation: effect of substrate and catalyst loading', *Catalysis Science & Technology*, 5: 3242-45.

Kumaniaev, Ivan, Elena Subbotina, Jonas Sävmarker, Mats Larhed, Maxim V. Galkin, and Joseph S. M. Samec. 2017. 'Lignin depolymerization to monophenolic compounds in a flow-through system', *Green Chemistry*, 19: 5767-71.

Langholtz, M. H.; Stokes, B. J.; Eaton, L. M. . 2016. "2016 Billion-Ton Report: Advancing Domestic Resources for a Thriving Bioeconomy." In, edited by U.S. Department of Energy, 448p. Oak Ridge, TN: Oak Ridge National Laboratory.

Lee, Jae-Hee, Eun-Gu Lee, Oh-Shim Joo, and Kwang-Deog Jung. 2004. 'Stabilization of Ni/Al2O3 catalyst by Cu addition for CO2 reforming of methane', *Applied Catalysis A: General*, 269: 1-6.

Li, Changzhi, Mingyuan Zheng, Aiqin Wang, and Tao Zhang. 2012. 'One-pot catalytic hydrocracking of raw woody biomass into chemicals over supported carbide catalysts: simultaneous conversion of cellulose, hemicellulose and lignin', *Energy Environ. Sci.*, 5: 6383-90.

Li, Yongdan, Jiuling Chen, Liu Chang, and Yongning Qin. 1998. 'The Doping Effect of Copper on the Catalytic Growth of Carbon Fibers from Methane over a Ni/Al2O3Catalyst Prepared from Feitknecht Compound Precursor', *Journal of Catalysis*, 178: 76-83.

Liao, Y. H., S. F. Koelewijn, G. Van den Bossche, J. Van Aelst, S. Van den Bosch, T. Renders, K. Navare, T. Nicolai, K. Van Aelst, M. Maesen, H. Matsushima, J. M. Thevelein, K. Van Acker, B. Lagrain, D. Verboekend, and B. F. Sels. 2020. 'A sustainable wood biorefinery for low-carbon footprint chemicals production', *Science*, 367: 1385-+.

Loe, Ryan, Yasmeen Lavoignat, Miranda Maier, Mohanad Abdallah, Tonya Morgan, Dali Qian, Robert Pace, Eduardo Santillan-Jimenez, and Mark Crocker. 2019. 'Continuous Catalytic Deoxygenation of Waste Free Fatty Acid-Based Feeds to Fuel-Like Hydrocarbons Over a Supported Ni-Cu Catalyst', *Catalysts*, 9.

Loe, Ryan, Eduardo Santillan-Jimenez, Tonya Morgan, Lilia Sewell, Yaying Ji, Samantha Jones, Mark A. Isaacs, Adam F. Lee, and Mark Crocker. 2016. 'Effect of Cu and Sn promotion on the catalytic deoxygenation of model and algal lipids to fuel-like hydrocarbons over supported Ni catalysts', *Applied Catalysis B: Environmental*, 191: 147-56.

Luo, Hao, Ian M. Klein, Yuan Jiang, Hanyu Zhu, Baoyuan Liu, Hilkka I. Kenttämaa, and Mahdi M. Abu-Omar. 2016. 'Total Utilization of Miscanthus Biomass, Lignin and Carbohydrates, Using Earth Abundant Nickel Catalyst', *Acs Sustainable Chemistry & Engineering*, 4: 2316-22.

Luque de Castro, M. D., and L. E. García Ayuso. 2000. 'ENVIRONMENTAL APPLICATIONS | Soxhlet Extraction.' in Ian D. Wilson (ed.), *Encyclopedia of Separation Science* (Academic Press: Oxford).

Minami, E., H. Kawamoto, and S. Saka. 2003. 'Reaction behavior of lignin in supercritical methanol as studied with lignin model compounds', *Journal of Wood Science*, 49: 158-65.

Minami, E., and S. Saka. 2003. 'Comparison of the decomposition behaviors of hardwood and softwood in supercritical methanol', *Journal of Wood Science*, 49: 0073-78.

Morgan, Tonya, Eduardo Santillan-Jimenez, Anne E. Harman-Ware, Yaying Ji, Daniel Grubb, and Mark Crocker. 2012. 'Catalytic deoxygenation of triglycerides to hydrocarbons over supported nickel catalysts', *Chemical Engineering Journal*, 189-190: 346-55.

Morton, S.A. Morton and L.A. 2010. 'Ionic Liquids for the Utilization of Lignocellulosics.' in M. Crocker (ed.), *Thermochemical Conversion of Biomass to Liquid Fuels and Chemicals* (RSC Publishing).

Narani, Anand, Ramesh Kumar Chowdari, Catia Cannilla, Giuseppe Bonura, Francesco Frusteri, Hero Jan Heeres, and Katalin Barta. 2015. 'Efficient catalytic hydrotreatment of Kraft lignin to alkylphenolics using supported NiW and NiMo catalysts in supercritical methanol', *Green Chemistry*, 17: 5046-57.

Ouyang, Xianhong, Xiaoming Huang, Jiadong Zhu, Michael D. Boot, and Emiel J. M. Hensen. 2019. 'Catalytic Conversion of Lignin in Woody Biomass into Phenolic Monomers in Methanol/Water Mixtures without External Hydrogen', *ACS Sustainable Chemistry & Engineering*, 7: 13764-73.

Park, Jaeyong, Asim Riaz, Deepak Verma, Hyun Jeong Lee, Han Min Woo, and Jaehoon Kim. 2019. 'Fractionation of Lignocellulosic Biomass over Core–Shell Ni@Al2O3 Catalysts with Formic Acid as a Cocatalyst and Hydrogen Source', *Chemsuschem*, 12: 1743-62.

Parsell, Trenton, Sara Yohe, John Degenstein, Tiffany Jarrell, Ian Klein, Emre Gencer, Barron Hewetson, Matt Hurt, Jeong Im Kim, Harshavardhan Choudhari, Basudeb Saha, Richard Meilan, Nathan Mosier, Fabio Ribeiro, W. Nicholas Delgass, Clint Chapple, Hilkka I. Kenttämaa, Rakesh Agrawal, and Mahdi M. Abu-Omar. 2015. 'A synergistic biorefinery based on catalytic conversion of lignin prior to cellulose starting from lignocellulosic biomass', *Green Chemistry*, 17: 1492-99.

Patterson, A. L. 1939. 'The Scherrer Formula for X-Ray Particle Size Determination', *Physical Review*, 56: 978-82.

Pepper, J. M., and Y. W. Lee. 1970. 'Lignin and related compounds. II. Studies using ruthenium and Raney nickel as catalysts for lignin hydrogenolysis', *Canadian Journal of Chemistry*, 48: 477-79.

Pepper, J. M., and Warren Steck. 1963. 'THE EFFECT OF TIME AND TEMPERATURE ON THE HYDROGENATION OF ASPEN LIGNIN', *Canadian Journal of Chemistry*, 41: 2867-75.

Pepper, James M., and Harold Hibbert. 1948. 'Studies on Lignin and Related Compounds. LXXXVII. High Pressure Hydrogenation of Maple Wood¹', *Journal of the American Chemical Society*, 70: 67-71.

Pirola, Carlo, Federico Galli, and Gregory S. Patience. 2018. 'Experimental methods in chemical engineering: Temperature programmed reduction-TPR', *The Canadian Journal of Chemical Engineering*, 96: 2317-20.

Ragauskas, Arthur J., Gregg T. Beckham, Mary J. Biddy, Richard Chandra, Fang Chen, Mark F. Davis, Brian H. Davison, Richard A. Dixon, Paul Gilna, Martin Keller, Paul Langan, Amit K. Naskar, Jack N. Saddler, Timothy J. Tschaplinski, Gerald A. Tuskan, and Charles E. Wyman. 2014. 'Lignin Valorization: Improving Lignin Processing in the Biorefinery', *Science*, 344: 709-+.

Renders, T., E. Cooreman, S. Van Den Bosch, W. Schutyser, S. F. Koelewijn, T. Vangeel, A. Deneyer, G. Van Den Bossche, C. M. Courtin, and B. F. Sels. 2018. 'Catalytic lignocellulose biorefining in n-butanol/water: a one-pot approach toward phenolics, polyols, and cellulose', *Green Chemistry*, 20: 4607-19.

Renders, T., S. Van Den Bosch, S. F. Koelewijn, W. Schutyser, and B. F. Sels. 2017. 'Lignin-first biomass fractionation: the advent of active stabilisation strategies', *Energy & Environmental Science*, 10: 1551-57.

Renders, T., S. Van den Bosch, T. Vangeel, T. Ennaert, S. F. Koelewijn, G. Van den Bossche, C. M. Courtin, W. Schutyser, and B. F. Sels. 2016. 'Synergetic Effects of Alcohol/Water Mixing on the Catalytic Reductive Fractionation of Poplar Wood', *Acs Sustainable Chemistry & Engineering*, 4: 6894-904.

Renders, T., G. Van den Bossche, T. Vangeel, K. Van Aelst, and B. Sels. 2019. 'Reductive catalytic fractionation: state of the art of the lignin-first biorefinery', *Current Opinion in Biotechnology*, 56: 193-201.

Rinaldi, Roberto, Robin Jastrzebski, Matthew T. Clough, John Ralph, Marco Kennema, Pieter C. A. Bruijnincx, and Bert M. Weckhuysen. 2016. 'Paving the Way for Lignin Valorisation: Recent Advances in Bioengineering, Biorefining and Catalysis', *Angewandte Chemie-International Edition*, 55: 8164-215.

Rinaldi, Roberto, Robert Woodward, Paola Ferrini, and Hebert Rivera. 2019. 'Lignin-First Biorefining of Lignocellulose: the Impact of Process Severity on the Uniformity of Lignin Oil Composition', *Journal of the Brazilian Chemical Society*.

Rosenfeld, J. 2018. "A Life-Cycle Analysis of the Greenhouse Gas Emissions from Corn-Based Ethanol." In. Washington, DC: Report prepared by ICF under USDA Contract No. AG-3142-D-17-0161.

Rynkowski, J. M., T. Paryjczak, and M. Lenik. 1993. 'On the nature of oxidic nickel phases in NiO/γ-Al2O3 catalysts', *Applied Catalysis A: General*, 106: 73-82.

Sankar, Meenakshisundaram, Nikolaos Dimitratos, Peter J. Miedziak, Peter P. Wells, Christopher J. Kiely, and Graham J. Hutchings. 2012. 'Designing bimetallic catalysts for a green and sustainable future', *Chemical Society Reviews*, 41: 8099.

Santillan-Jimenez, Eduardo, Ryan Loe, Makaylah Garrett, Tonya Morgan, and Mark Crocker. 2018. 'Effect of Cu promotion on cracking and methanation during the Ni-catalyzed deoxygenation of waste lipids and hemp seed oil to fuel-like hydrocarbons', *Catalysis Today*, 302: 261-71.

Schutyser, W., T. Renders, S. Van den Bosch, S. F. Koelewijn, G. T. Beckham, and B. F. Sels. 2018. 'Chemicals from lignin: an interplay of lignocellulose fractionation, depolymerisation, and upgrading', *Chemical Society Reviews*, 47: 852-908.

Schutyser, W., S. Van den Bosch, T. Renders, T. De Boe, S. F. Koelewijn, A. Dewaele, T. Ennaert, O. Verkinderen, B. Goderis, C. M. Courtin, and B. F. Sels. 2015. 'Influence of bio-based solvents on the catalytic reductive fractionation of birch wood', *Green Chemistry*, 17: 5035-45.

Schutyser, Wouter, Tom Renders, Gil Van den Bossche, Sander Van den Bosch, Steven-Friso Koelewijn, Thijs Ennaert, and Bert F. Sels. 2017. 'Catalysis in Lignocellulosic Biorefineries: The Case of Lignin Conversion.' in, *Nanotechnology in Catalysis*.

Sharma, G., D. Kumar, A. Kumar, A. H. Al-Muhtaseb, D. Pathania, M. Naushad, and G. T. Mola. 2017. 'Revolution from monometallic to trimetallic nanoparticle composites, various synthesis methods and their applications: A review', *Mater Sci Eng C Mater Biol Appl*, 71: 1216-30.

Shen, Dekui, Chongbo Cheng, Nana Liu, and Rui Xiao. 2016. 'Lignin Depolymerization (LDP) with Solvolysis for Selective Production of Renewable Aromatic Chemicals.' in Zhen Fang and Jr Richard L. Smith (eds.), *Production of Biofuels and Chemicals from Lignin* (Springer Singapore: Singapore).

Smith, D. C. C. 1955. 'p-Hydroxybenzoate groups in the lignin of aspen (populus tremula)', *Journal of the Chemical Society (Resumed)*: 2347-51.

Song, Qi, Feng Wang, Jiaying Cai, Yehong Wang, Junjie Zhang, Weiqiang Yu, and Jie Xu. 2013. 'Lignin depolymerization (LDP) in alcohol over nickel-based catalysts via a fragmentation–hydrogenolysis process', *Energy & Environmental Science*, 6: 994.

Song, Yang. 2019. 'Lignin Valorization via Reductive Depolymerization.' in.

Stone, Michael L., Eric M. Anderson, Kelly M. Meek, Michelle Reed, Rui Katahira, Fang Chen, Richard A. Dixon, Gregg T. Beckham, and Yuriy Román-Leshkov. 2018. 'Reductive Catalytic Fractionation of C-Lignin', *ACS Sustainable Chemistry & Engineering*, 6: 11211-18.

Stone, Michael L., Matthew S. Webber, William P. Mounfield, David C. Bell, Earl Christensen, Ana R. C. Morais, Yanding Li, Eric M. Anderson, Joshua S. Heyne, Gregg T. Beckham, and Yuriy Román-Leshkov. 2022. 'Continuous hydrodeoxygenation of lignin to jet-range aromatic hydrocarbons', *Joule*.

Sultan, Zafar, Inês Graça, Yueqin Li, Sérgio Lima, Ludmila G. Peeva, Daeok Kim, Mahmood A. Ebrahim, Roberto Rinaldi, and Andrew G. Livingston. 2019. 'Membrane Fractionation of Liquors from Lignin-First Biorefining', *Chemsuschem*, 12: 1203-12.

Sun, Zhuohua, Giovanni Bottari, Anastasiia Afanasenko, Marc C. A. Stuart, Peter J. Deuss, Bálint Fridrich, and Katalin Barta. 2018. 'Complete lignocellulose conversion with integrated catalyst recycling yielding valuable aromatics and fuels', *Nature Catalysis*, 1: 82-92.

Sun, Zhuohua, Zhe-Hui Zhang, Tong-Qi Yuan, Xiaohong Ren, and Zeming Rong. 2021. 'Raney Ni as a Versatile Catalyst for Biomass Conversion', *ACS Catalysis*, 11: 10508-36.

Tyner, Wallace E., and Farzad Taheripour. 2014. 'Advanced Biofuels: Economic Uncertainties, Policy Options, and Land Use Impacts.' in Maureen C. McCann, Marcos S. Buckeridge and Nicholas C. Carpita (eds.), *Plants and BioEnergy* (Springer New York: New York, NY).

Van Aelst, K., E. Van Sinay, T. Vangeel, E. Cooreman, G. Van den Bossche, T. Renders, J. Van Aelst, S. Van den Bosch, and B. F. Sels. 2020. 'Reductive catalytic fractionation of pine wood: elucidating and quantifying the molecular structures in the lignin oil', *Chemical Science*, 11: 11498-508.

Van den Bosch, S., T. Renders, S. Kennis, S. F. Koelewijn, G. Van den Bossche, T. Vangeel, A. Deneyer, D. Depuydt, C. M. Courtin, J. M. Thevelein, W. Schutyser, and B. F. Sels. 2017.

'Integrating lignin valorization and bio-ethanol production: on the role of Ni-Al2O3 catalyst pellets during lignin-first fractionation', *Green Chemistry*, 19: 3313-26.

Van Den Bosch, S., W. Schutyser, S. F. Koelewijn, T. Renders, C. M. Courtin, and B. F. Sels. 2015. 'Tuning the lignin oil OH-content with Ru and Pd catalysts during lignin hydrogenolysis on birch wood', *Chemical Communications*, 51: 13158-61.

Van den Bosch, S., W. Schutyser, R. Vanholme, T. Driessen, S. F. Koelewijn, T. Renders, B. De Meester, W. J. J. Huijgen, W. Dehaen, C. M. Courtin, B. Lagrain, W. Boerjan, and B. F. Sels. 2015. 'Reductive lignocellulose fractionation into soluble lignin-derived phenolic monomers and dimers and processable carbohydrate pulps', *Energy & Environmental Science*, 8: 1748-63.

Verhaak, M. J. F. M., A. J. van Dillen, and J. W. Geus. 1993. 'Measuring the acid-base properties of supported nickel catalysts using temperature-programmed desorption of ammonia', *Applied Catalysis A: General*, 105: 251-69.

Vizcaíno, A. J., A. Carrero, and J. A. Calles. 2007. 'Hydrogen production by ethanol steam reforming over Cu–Ni supported catalysts', *International Journal of Hydrogen Energy*, 32: 1450-61.

Wang, Lei, Dalin Li, Mitsuru Koike, Shuichi Koso, Yoshinao Nakagawa, Ya Xu, and Keiichi Tomishige. 2011. 'Catalytic performance and characterization of Ni-Fe catalysts for the steam reforming of tar from biomass pyrolysis to synthesis gas', *Applied Catalysis A: General*, 392: 248-55.

Yan, Ning, Chen Zhao, Paul J Dyson, Chen Wang, Ling-Tao Liu, and Yuan Kou. 2008. 'Selective Degradation of Wood Lignin over Noble-Metal Catalysts in a Two-Step Process', *Chemsuschem*, 1: 626-29.

Yang, Haibing, Ximing Zhang, Hao Luo, Baoyuan Liu, Tânia M. Shiga, Xu Li, Jeong Im Kim, Peter Rubinelli, Jonathan C. Overton, Varun Subramanyam, Bruce R. Cooper, Huaping Mo, Mahdi M. Abu-Omar, Clint Chapple, Bryon S. Donohoe, Lee Makowski, Nathan S. Mosier, Maureen C. McCann, Nicholas C. Carpita, and Richard Meilan. 2019. 'Overcoming cellulose recalcitrance in woody biomass for the lignin-first biorefinery', *Biotechnology for Biofuels*, 12.

Yang, Hong, and Jerry L. Whitten. 1993. 'Dissociative adsorption of H₂ on Ni(111)', *The Journal of Chemical Physics*, 98: 5039-49.

Yu, Weiting, Marc D. Porosoff, and Jingguang G. Chen. 2012. 'Review of Pt-Based Bimetallic Catalysis: From Model Surfaces to Supported Catalysts', *Chemical Reviews*, 112: 5780-817.

Yu, Xinbin, Jixiang Chen, and Tianyu Ren. 2014. 'Promotional effect of Fe on performance of Ni/SiO2 for deoxygenation of methyl laurate as a model compound to hydrocarbons', *RSC Advances*, 4: 46427-36.

Zakzeski, Joseph, Pieter C. A. Bruijnincx, Anna L. Jongerius, and Bert M. Weckhuysen. 2010. 'The Catalytic Valorization of Lignin for the Production of Renewable Chemicals', *Chemical Reviews*, 110: 3552-99.

Zhai, Yongxiang, Chuang Li, Guangyue Xu, Yanfu Ma, Xiaohao Liu, and Ying Zhang. 2017. 'Depolymerization of lignin via a non-precious Ni–Fe alloy catalyst supported on activated carbon', *Green Chemistry*, 19: 1895-903.

Zhang, Liming, and Göran Gellerstedt. 2001. 'NMR observation of a new lignin structure, a spiro-dienoneElectronic supplementary information (ESI) available: 13C, QUAT, HMBC and HSQC NMR spectra. See http://www.rsc.org/suppdata/cc/b1/b108285j', *Chemical Communications*: 2744-45.

Zieliński, Jerzy. 1982. 'Morphology of nickel/alumina catalysts', *Journal of Catalysis*, 76: 157-63.

VITA

Julia E. Parker

Education

Master of Science in Biosystems and Agricultural Engineering,
University of Kentucky, Expected 2022

Graduate Certificate: Innovation at the Nexus of Food, Energy, & Water Systems,
University of Kentucky, Expected 2022

Bachelor of Science in Biosystems and Agricultural Engineering,
University of Kentucky, 2019

Professional and Research Experience

Graduate Research Assistant, Center for Applied Energy Research,
University of Kentucky, Lexington, KY (08/2019 – 07/2022)

Undergraduate Research Assistant, Center for Applied Energy Research,
University of Kentucky, Lexington, KY (07/2018 – 08/2019)

Professional Affiliations

American Chemical Society (ACS)

Society for the Advancement of Chicanos/Hispanics and Native Americans in Science (SACNAS)

Kentucky-West Virginia Louis Stokes Alliance for Minority Participation
(KY-WV LSAMP)

Awards and Honors

Bridge to Doctorate Fellowship. *National Science Foundation*. 2019 – 2022.

Dean's List. *University of Kentucky.* Spring 2019.

Bluegrass Spirit Scholarship. *University of Kentucky.* 2014 – 2018.

William C. Parker Scholarship. *University of Kentucky.* 2014 – 2018.